A review of recent advances in adsorption desalination technologies

Nadia Riaz[a,†], Muhammad Sultan[a,†,*], Takahiko Miyazaki[b,c], Muhammad W. Shahzad[d], Muhammad Farooq[e], Uzair Sajjad[f], Yasir Niaz[g]

[a]Laboratory for Energy and Env. Engineering Research, Department of Agricultural Engineering, Bahauddin Zakariya University, Multan 60800, Pakistan

[b]Department of Advanced Environmental Science and Engineering, Faculty of Engineering Sciences, Kyushu University, Fukuoka 816-8580, Japan

[c]International Institute for Carbon-Neutral Energy Research (WPI-I2CNER), Kyushu University, 744 Motooka, Nishi-ku, Fukuoka 819-0395, Japan

[d]Department of Mechanical and Construction Engineering, Northumbria University, Newcastle Upon Tyne, NE1 8ST, United Kingdom

[e]Department of Mechanical Engineering, University of Engineering and Technology, 39161 Lahore, Pakistan

[f]Mechanical Engineering Department, National Chiao Tung University, Hsinchu, Taiwan

[g]Department of Agricultural Engineering, Khwaja Fareed University of Engineering & Information Technology, Rahim Yar Khan, 64200, Pakistan

[†] These authors contributed equally to this work.

[*]Correspondence: muhammadsultan@bzu.edu.pk ; sultan@kyudai.jp

Abstract

Adsorption-based desalination (AD) is an emerging concept to co-generate distilled fresh water and cooling applications. The present study is aimed to provide a comprehensive review of the adsorption desalination systems and subsequent hybridization with known conventional cycles such as the multiple-effect AD (MED), solar regenerable, integrated evaporator-condenser cascaded, and ejector integrated systems. The systems are investigated for energy consumption, productivity enhancement, and performance parameters, including production cost, daily water production, and performance coefficient. Comprehensive economic aspects, future challenges, and future progress of the technologies are discussed accordingly to pave researchers' paths for technological innovation. Traditional AD systems can produce specific daily water production of 25 kg per kg of adsorbent. The solar adsorption desalination-cooling (ADC) showed a promising specific cooling power of 112 W/kg along with a COP of 0.45. Furthermore, for a hybrid MEDAD cycle, the gain output ratio (GOR) and performance ratio (PR) is found to be 40%, along with an augmented water production rate from 60% to two folds. The AD technology could manage the

high salinity feed water with the production of low salinity water with a reasonable cost of US\$0.2/m^3.

Keywords: Adsorption desalination; adsorbent-adsorbate pairs; technologies; economic aspects; system performance.

Table of Contents

List of abbreviations

$\dot{Z}_k$	capital investment cost of the component k
AD	adsorption desalination
ADC	adsorption desalination-cooling
ADEJ	adsorption cooling/ejector system
ADS	adsorption desalination system
ADVC	adsorption vapor compression
C	adsorption capacity (kg/kg)
C_e	adsorbate concentration at equilibrium (mg/L)
CFD	computational fluid dynamics
C_o	maximum adsorption capacity (kg/kg)
COP	coefficient of performance [-]
C_p	specific heat (kJ/kg)
CR	compression ratio
CRF	capital recovery factor
DEARC	double ejector refrigeration cycle
D_{so}	pre-exponential coefficient (m^2/s)
E_a	activation energy (kJ/mol)
EC	electrical conductivity (S/m)
EPA	environmental protection agency
ER	ejector refrigeration
EVCC	ejector vapor compression cycle
GOR	gain output ratio
g_{sw}	specific Gibbs energy of seawater
h	enthalpy (kJ/kg)
h_{fg}	average radius of adsorption particles (m)
HVCR	hybrid vapor compression refrigeration system
K	partition coefficient (L/g)
K_0	pre-exponential constant
KAUST	King Abdullah University of Science and Technology
LBT	low-brine temperature (°C)

LCC	life cycle costing ($)
m	mass (kg)
M	molar mass (kg/mol)
$\dot{m}$	mass flow rate (kg/s)
MC	merocyanine
MED	multiple-effect distillation
MED-AD	multi effect desalination and adsorption desalination
MSF	multi-stage flash distillation
NF	nanofiltration
NUS	National University of Singapore
OCR	overall conversion ratio
ORC	organic Rankine cycle
PR	performance ratio
Q	heat energy (W)
q_e	adsorbed amount (mg/g)
RO	reverse osmosis
SCC	stress corrosion cracking
SCP	specific cooling power (TR/ton of adsorbent)
SDWP	specific daily water production (kg/kg adsorbent/day)
SP	spiropyran
T	temperature (K)
t	time (s)
t_{cycle}	cycle time (s)
TBT	top-brine temperature (°C)
TC	total carbon
TDS	total dissolved solids (mg/l)
TOC	total organic carbon
UPR	universal performance ratio
AD2EJ	adsorption desalination/2 ejectors system
UV	ultraviolet
VCC	vapor compression cycle

VCR	vapor compression refrigeration system
VCSC	vapor compression sub-cycle
ΔH_{ads}	isosteric enthalpy of adsorption
μ_0	chemical potential
τ	total annual time of system operation (hours)

Subscripts/superscripts

cu	copper
d	desalinated
des	desorption
i_{eff}	average annual effective discount rate
in	inlet
out	outlet
sg	silica-gel
sw	sea water

1. Introduction

Water scarcity and its unbridled contamination are pressing issues that inscribe the world population to curb this grave scenario. By 2050, around 6 billion population is expected to be afflicted by water scarcity [1]. Freshwater is an exiguous resource that makes up only 0.75% of the total quantity on earth readily available for human consumption, and 7.75% is stored in glaciers and ice caps, while the remaining 97.5% is saline water [2]. The exponential population growth, urbanization, rapid industrialization, climate change, and contamination of freshwater resources pose a threat and lead towards a severe global challenge to ample provision of potable freshwater [3]. It is high time to address the issue and consider the solemnness of posed challenges in this situation. Existing resources of freshwater do not satisfy the water consumption patterns. It is hence escalating the demand for freshwater. Alternative methods are employed to surmount the challenges. It is rudimentary to address the water scarcity with saline water desalination. Therefore, this method has been scientifically proved to be worth adopting, and the water industry has become increasingly reliant on desalination techniques as it could be the most feasible option. The desalination technique has evolved as a non-conventional alternate to counteract the challenge of scarce freshwater resources by efficiently using abundant saline water resources [4]. The global daily desalination capacity is 95 million cubic meters/day (MCM/d) or 38 billion cubic meters (BCM/yr.) with an annual consumption of 75.2 TWh [5]. Researches have been carried out, resulting in various membrane and thermal distillation systems to satisfy the water requirements. According to a study by OECD [6], the global water demand is projected to escalate from 3500 km^3 to 5500 km^3 from 2000 to 2050, which records an increment of 55%, as presented in Fig. 1. The manufacturing industry is found to be the primary cause of growing demand.

The variation in water utilization pattern disrupts the global water demand as a large amount is returned to the mainstream after use. Thus, depending on the quality of water, the remaining quantity is offered to be used downstream. It is also projected that by 2050, with the lack of new policies, there will be a significant shift in water use, causing water demand [6]. The growing water demand can be addressed by the desalination of seawater or treating the wastewater. Seawater desalination can be the ultimate suitable process for some countries where direct wastewater reuse is insufficient to fill the shortfall. In the past 20 years, the rise in the adoption of desalination technology has opened doors to satisfy the global water demand. It is expected that the installation and adoption of desalination technologies will be two folds by 2030, as shown in Fig. 2. Currently, 19,500 desalination plants are operating in 150 countries, having a production capacity of 100 million m^3/day, against the demand of 300 million people globally [7].

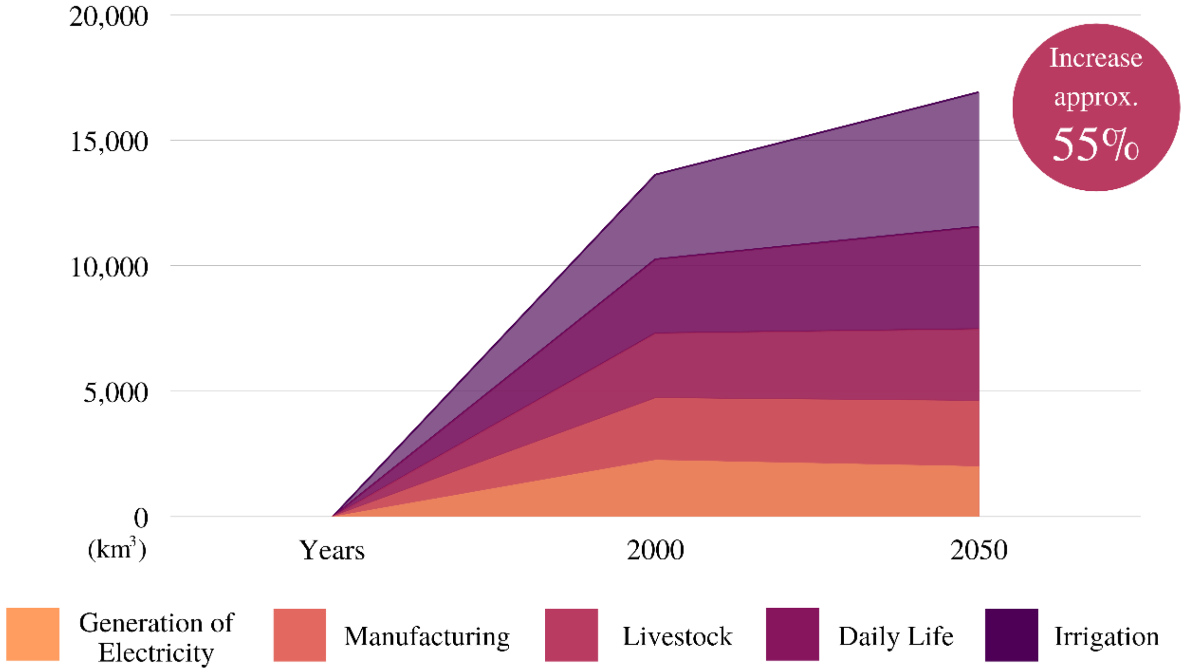

Fig. 1. Global blue water demand from 2000 to 2050, reproduced from [6].

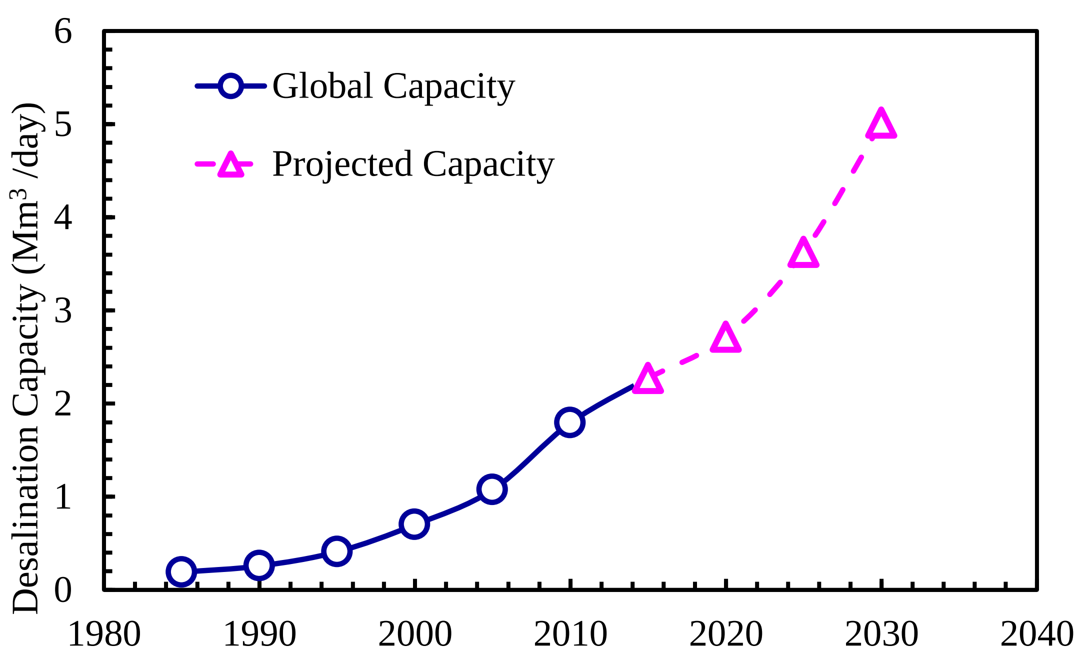

Fig. 2. Global desalination capacity of installed desalination technologies, trend, and projection from 1985 to 2030, reproduced from [7].

The technologies are classified, such as thermal desalination system that includes multi-stage flash (MSF) or multi-effect distillation, providing around 18% and 17% of the global desalination capacity. However, the membrane desalination systems include nano-filtration (NF) and reverse osmosis (RO) that employ 3% and 69% of the global desalination capacity, respectively [8]. These technologies are mainly adopted for large capacities [9], and most large-scale systems such as RO and MSF are driven by fossil fuels having a large carbon footprint. The adsorption desalination showed distinguished advantages over the other desalination options, which includes: (i) ability to utilize solar heat or low-grade waste energy at a temperature lower than 100°C, (ii) reduced maintenance cost due to simple construction and no significant moving parts, (iii) opportunity to use commonly available environment-friendly adsorbent/adsorbate pairs, i.e., silica gel/water, (iv) zero carbon footprint and emission reduction for greenhouse gases, (v) employment of controlled corrosion and fouling rate on evaporator tubes material due to accruing of seawater evaporation at comparatively reduced temperature (around < 35°C), (vi) the ability to cogenerate freshwater along with cooling power, (vii) reduced electricity consumption of about 1.0-1.5 kW/m^3 [10–15]. The refrigeration technologies, along with their manufacturers, are summarized in Fig. 3. Several companies manufacture solar refrigeration machines using adsorption/absorption concepts with a power rating ranging from 5 kW to 200 kW. The most commercialized systems possess the power of less than 50 kW and employ H_2O/LiBr operating fluid and falling in the category of absorption technology. The technologies mainly presented belong to German or Asian markets [16].

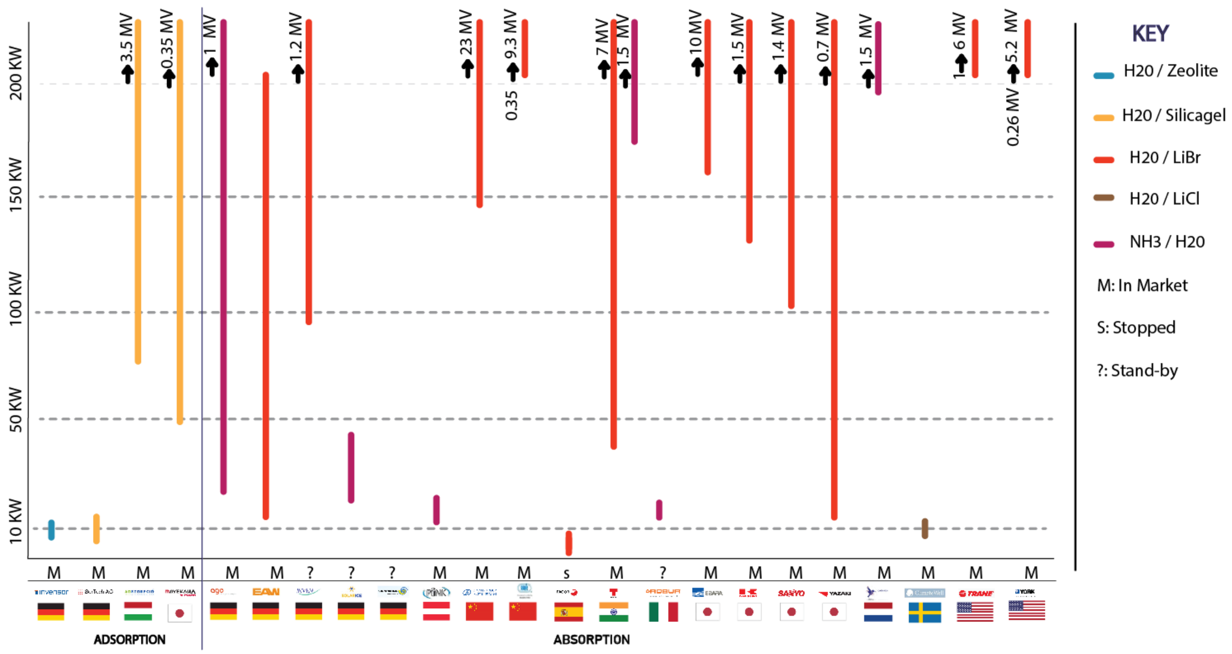

Fig. 3. A general representation of solar refrigeration technologies and associated power rating using adsorption/absorption concepts with their subsequent global manufacturers, reproduced from [16].

Apart from the benefits, the AD technologies possess some drawbacks of low system performance in terms of cooling capacity and COP. As a result, it has received little consideration from researchers in the past but has recently gained considerable importance because of its ability to be separable at low temperatures from driving heat source temperatures [17–20]. For example, desiccant air-conditioning (AC) involves adsorbate and water for the dehumidification process of process air [21,22]. The central systems included are desiccant [23–25], adsorption [26–28], and absorption technologies [29–32].

In 1984, one of the earliest units of adsorption desalination system was reported by Broughton [33][10]. It was a two-bed thermal adsorption desalination system for which simulations were performed. Several other developments were also made with the purpose of performance enhancement of the system. Zejli et al. [10,14] reported a multi-effect desalination (MED) system coupled with an adsorption heat pump utilizing zeolite/water pair. The heat pump coupled multi-effect desalination unit uses internal heat recovery to supply steam and seawater to the MED unit. A three-effect desalination system design with an evaporator sandwiched between two adsorption beds was proposed [10]. In this regard, the second bed utilizes the heat rejected from one bed directly without processing because the second bed needs high-temperature thermal energy. Ng et al. [10,13], and Wang and Ng [15] have presented the performance evaluation of a four-bed adsorption desalination plant using silica gel/water. The same research group has reported specific daily water production of 4.7 kg per kg of silica gel for an adsorption desalination plant utilizing cooled water [13].

The adsorption desalination (AD) cycle works on two main processes: (i) the adsorption-evaporation process and (ii) the desorption-condensation process [10,34–39]. In the first cycle of the process, the adsorbent absorbs the vapors generated in the evaporator. Seawater is sprayed over the tube bundle in the evaporator while the refrigerant circulation occurs [40]. The two significant outputs are produced simultaneously by the adsorption cooling and desalination cycle. These outputs are obtained using a multi-bed arrangement [10,41]. It is to note that the closed cycles of air and water aids to significantly increase the energy recovery since the energy provided as input is utilized to heat water and is preserved during the process [42]. The gas and water valve delay ensures a conventional heat recovery scheme [43]. There is another type of energy recovery scheme that involves both mass and heat recovery processes. The second category is attained through the pressure equalization process for the pre-cooling and pre-heating beds. Hence, the adsorption and desorption processes are both improved [15,43–46]. The brine lowers the input energy requirement for feedwater heating, and then processed air is used for preheating water within the dehumidifier. Heat recovery in an advanced AD cycle is attained either by the water run around the condenser and evaporator or a device consisting of an enclosed evaporator and condenser [47–50]. Despite the large consumption of energy, reduced productivity has gained researchers' attention. Thereby, a few solutions are discussed accordingly in this study.

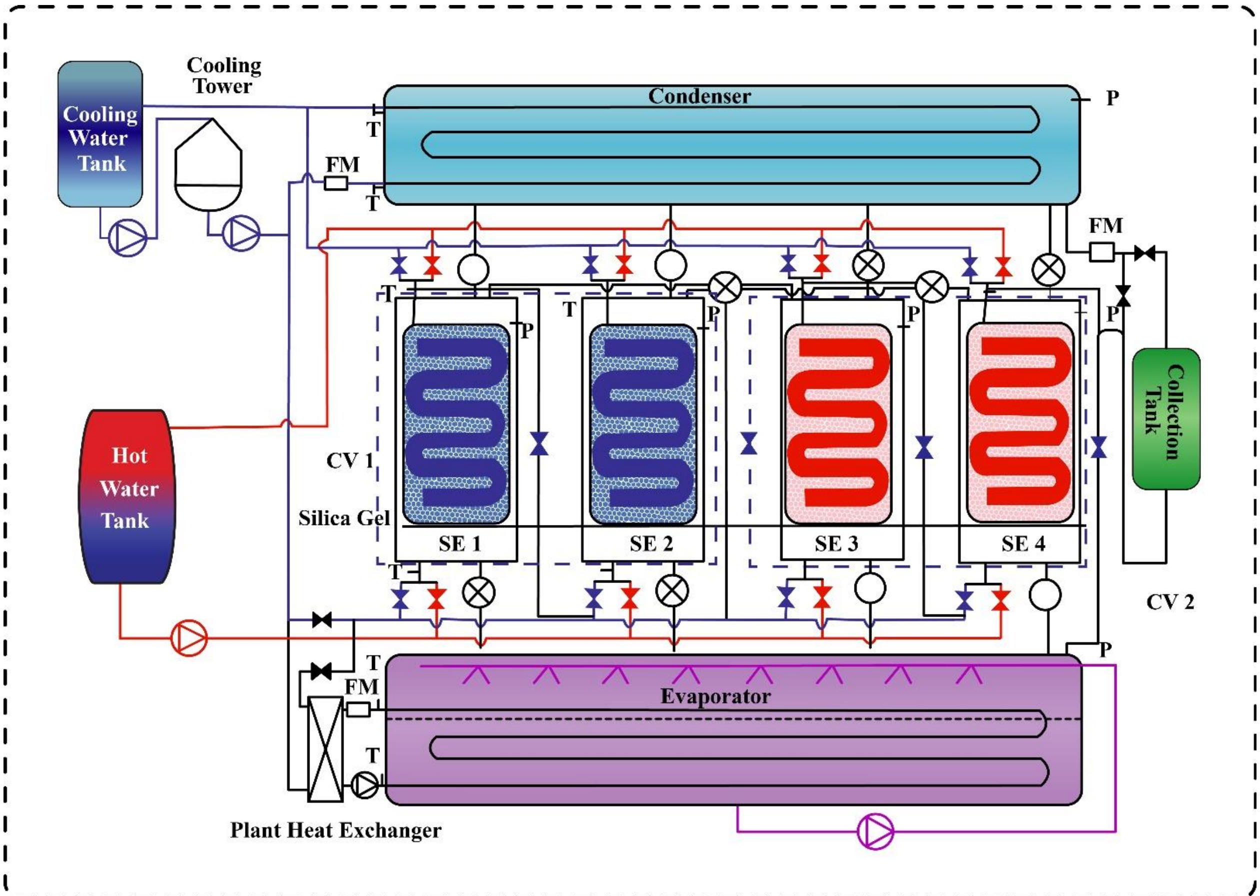

Fig. 4. Schematic diagram of a conventional adsorption desalination system.

The conventional adsorption desalination system is shown in Fig. 4, which consists of three major design components, i.e. (i) copper-nickel or stainless steel evaporator to prevent erosion, (ii) the reactor consisting of silica gel packed heat exchanger tubes, and (iii) condenser for water vapors condensation. The desalination system requires an intrinsic minimum available energy and is known to be an energy-intensive process [43,51–53].

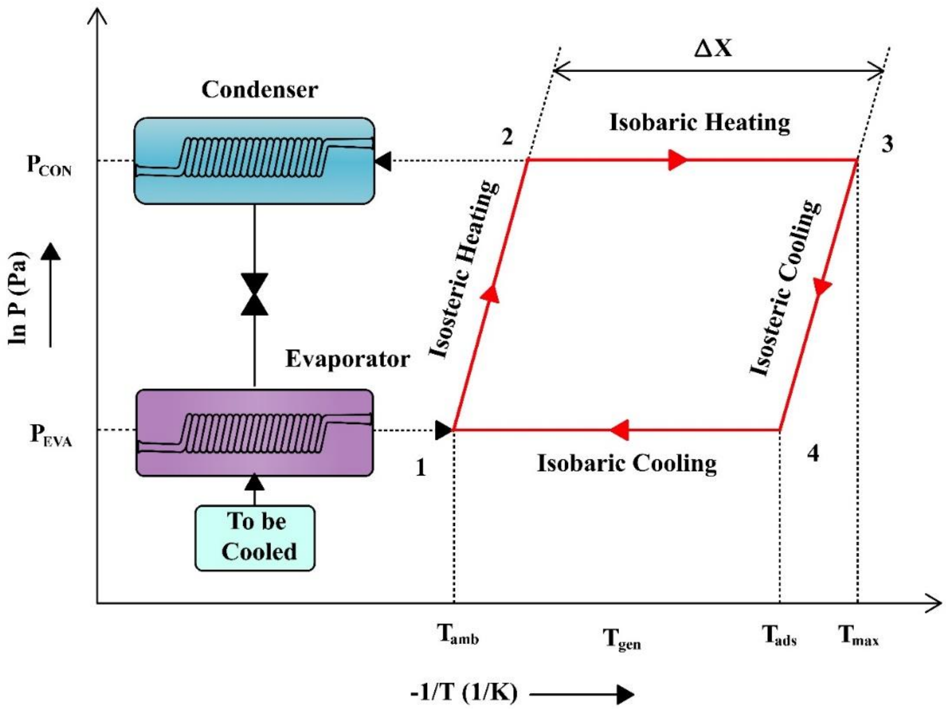

Fig. 5. A fundamental (PTX) diagram of an adsorption desalination thermodynamic cyclic process.

A thermodynamic cyclic process for an adsorption desalination system is represented in Fig. 5. First, the process from 1 to 2 undergoes an isosteric heating process, which goes to desorption from processes 2 to 3, also known as the isobaric heating process. Then, the isosteric heating occurs from 3 to 4, followed by adsorption, known as isobaric cooling. The PTX diagram is presented where -1/T is plotted on the x-axis and lnP is plotted on the y-axis. Where X is the amount (kg of adsorbate per kg of adsorbent) of adsorbed adsorbate by the adsorbent at equilibrium conditions, it is helpful to depict the thermodynamic cycle of an adsorption desalination system (ADS), where X_{min}, X_{max}, T_{ads}, and T_{gen} represent the minimum and maximum amount of water adsorbed and the temperature at which the desorption and adsorption process takes place, respectively [54].

Adsorption working pairs, e.g., silica gel-water, are the necessitous components in the adsorption system. While comparing silica gel-water and zeolite-water adsorption working pairs, silica gel has a structure of dehydrated polymeric colloidal silica acid along with the pattern of SiO_2. nH_2O. The spherical particles of amorphous material are 2-20 nm in size, which form the silica by sticking with each other [55]. Silica gel is a preferred adsorbent due to its ability to take up a reasonable amount of water (up to 40% by mass) [56] without considerable change in volume or structure and capacity to release water when mildly heated [57]. Systems with two or more beds are used in the literature [58] regarding the improvement in energy efficiency, and several studies have also reviewed AD systems.

For instance, a technical review [58] is presented on MSF and MED desalination configurations and processes, along with prevalent adsorption mechanisms and low-cost adsorbent materials. The regeneration of saturated adsorbent and study of the physisorption or different mechanisms for effective adsorption is recommended. Ng et al. [59] reported low-cost thermal desalination systems based on pilot-scale experiments and life cycle cost analysis. The study recommends life cycle costing (LCC) for the comparison of desalination technologies. Shahzad et al. [60] have also studied the recent developments of the AD theory cycle and conventional MED-AD cycles. The study analyzed different MED cycles while highlighting the critical role of AD cycle hybridization with proven cycles, i.e., the MED cycle. For significant improvement in the yield of water production, it is concluded that the UPR of the MED-AD cycle is the highest of all technologies with furthermore projection of lowered water production LCC. Analysis of various AD systems [10] for productivity improvements and proposed solutions for improving system and energy efficiency is performed. Accordingly, recently developed working pairs used in different configurations of AD systems are compared. Cooling power and water production mainly depend on the adsorbent's adsorption rate and adsorptive ability, making the working pair a crucial design parameter. Technological advancements in renewable energy sources assisted AD systems were investigated [34]. It reports the different adsorption desalination-cooling systems, solar thermal energy driven by ADS, waste heat-driven adsorption cooling cum desalination cycle, and AD cycle with internal preheat recovery.

A review on adsorption working pairs for adsorption cooling was presented in 2009 [61]. Accordingly, the study of composite adsorbents [62–64] was boosted about 20 years ago [65] with the aim to improve the heat/mass transfer performance by the adsorbents [63,64,66,67]. With the combination of some porous material and the chemical adsorbent yields, these adsorbents such as carbon fiber, activated carbon, graphite are commonly employed [63,68]. Similarly, a study was conducted for the investigation of water vapor adsorption capacity onto activated carbon fiber (ACF), activated carbon powder (ACP), and silica-gel [69]. As a result, the silica gel found an appropriate adsorbent for desalination [69].

Consequently, the thermophysical properties of commonly used adsorbents are presented in Table 1. Extensive studies have been carried out to investigate adsorption isotherms of various pairs [22,41,48,59,70–79]. The fundamental equations of adsorption isotherm models are summarized as presented in Table A1. It can be observed in the literature that there is a distinction in the adsorption mechanisms exhibited by different isotherm models. The possible adsorption mechanisms are unknown, and thereby the isotherms aids in the determination of adsorption mechanisms. Consequently, this study deals with the theoretical and experimental understanding of adsorption desalination technologies concerning performance parameters, comparative analysis, economic aspects, and future challenges.

Table 1. The thermophysical properties of commonly used adsorbents in the literature for adsorption desalination.

Working Pair	BET surface area (m^2/g)	Pore volume (m^3/kg)	Pore diameter (nm)	Maximum capacity (kg/kg)	Reference
Silica gel 2560/water	636.4	3.27×10^{-4}	1.32	0.32	[70]
Silica gel RD/water	838	4.0×10^{-4}	2.20	0.30	[80]
Fuji silica gel 2060/water	707	3.4×10^{-4}	1.92	0.37	[39]
Fuji silica gel RD/water	780	4.4×10^{-4}	2.24	0.48	[39]
Silica gel A^{++}/water	863.6	4.89×10^{-4}	1.38	0.48	[70]
AQSOA-Z05/water	187.1	0.7×10^{-4}	1.176	0.22	[81]
AQSOA-Z01/water	189.6	0.712×10^{-4}	1.178	0.215	[81]
Zeolite/water	643	3.1×10^{-4}	1.78	0.25	[82]
AQSOA-	717.8	2.69×10^{-4}	1.184	0.29	[81]

Z02/Water					

2. Performance of adsorption desalination system (ADS)

For achieving higher desalination rates and less energy consumption, conventional adsorption and desalination systems can be modified by applying mass and heat energy processes, improving the significant components, and compiling renewable energy sources. There are three indicators to describe the system performance, which indicate the cycle's productivity in cooling, desalination, and both. The specific daily water production (SDWP) and performance ratio (PR) are the parameters used for the calculation of the desalination coefficient of performance (COP) and specific cooling power (SCP) in the case of cooling. The overall conversion ratio (OCR) is the ratio between useful effects produced for the overall cycle system performance. Third, the summation of the heat of evaporation and heat of condensation over the input is the heat of desorption [48,79]. These parameters are presented in the equations (1-5) as given by [40] [73]:

$$COP = \int_0^{t\ cycle} \frac{Q_{evap}\tau}{Q_{des}} dt \tag{1}$$

$$SDWP = \int_0^{t\ cycle} \frac{Q_{cond}\tau}{h_{fg}\,(T_{cond})M_{sg}} dt \tag{2}$$

$$SCP = \int_0^{t\ cycle} \frac{Q_{evap}\tau}{M_{sg}} dt \tag{3}$$

$$PR = \int_0^{t\ cycle} \frac{\dot{m}_d\, h_{fg}\,(T_{cond})\tau}{(Q_{des})} dt \tag{4}$$

$$OCR = \int_0^{t\ cycle} \frac{Q_{evap}\ + Q_{cond}}{Q_{des}} dt \tag{5}$$

where Q_{evap}, Q_{des}, Q_{cond}, cycle time (s), and time (s) are shown in the nomenclature. Similarly, h_{fg} is the average radius of adsorption particles (m), M_{sg} is the mass of seawater, T_{cond} is the temperature of the condenser, and $\dot{m}_d$ is the desalination rate. The system performance improves, and adsorption of more adsorbent results as adsorption pressure increases. The heat recovery from beds to evaporator and condenser also results in increased evaporator and condenser profiles. The performance parameters drawn by theoretical and/or experimental study undergo the system evaluation without considering system energy loss by the components or process.

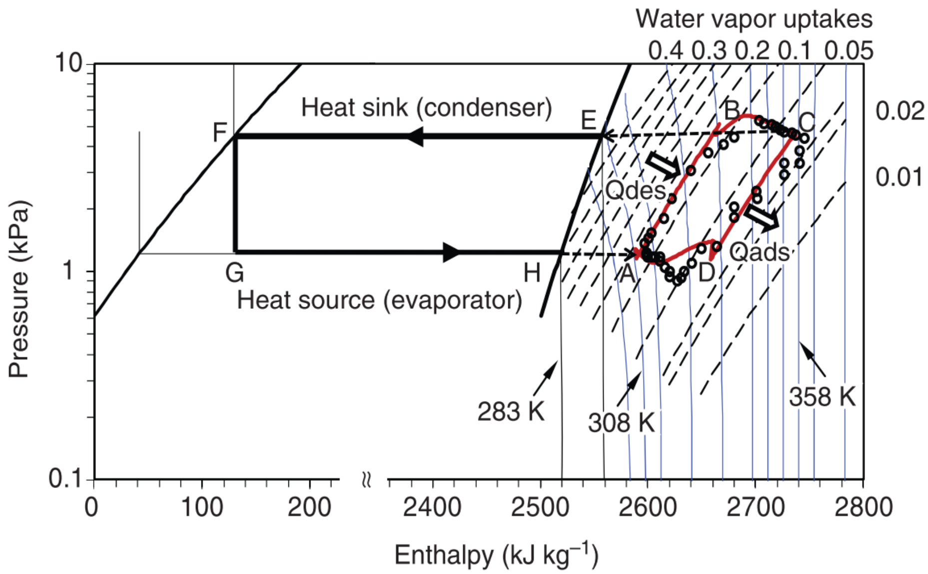

Fig. 6. Graphical representation of pressure (P) versus enthalpy (h) for adsorption desalination cycle [83].

It is relatively viable to determine the energetic performances of adsorption cycles from Fig. 6 regarding water production and cooling capacity. The enthalpy of evaporation h_{fg} (h_g - h_f) evolves at the evaporator due to the cooling load (Q_{evap}), and the silica gel surfaces of the sorption bed absorb the evaporated water vapor [83]. The adsorption cooling systems were analyzed based on exergy losses due to the thermodynamic parameters reported by Ngoc Vi Cao and Jae Dong Chung [84]. The CFD used yielded the results of anergy analysis. Based on the comprehensive information obtained from CFD results, the exergy analysis was carried out. The results revealed that increased energy performance is obtained when the temperature of the heat source increases.

Consequently, exergy analysis can be conducted for the complete performance evaluation. However, the energy available is rudimentary for estimating natural resource utilization, process economics, and environmental impacts based on environmental conditions [85,86]. Therefore, the determination of exergy and exergetic efficiency can be calculated from the equations (6) and (7) as given by [87][88] as:

$$e_f = (h - h^*) - T_o(s - s^*) + \sum_{i=1}^{n} w_i\,({\mu_i}^* - {\mu_i}^o) \quad (6)$$

$$E_{etha} = \dot{Q}_{evap}\left(1 - \frac{T_o}{T_{evap}}\right)/\dot{Q}_{des}\left(\frac{T_o}{T_{des}}\right) \quad (7)$$

The physical exergy is denoted by the first two terms, whereas the third term represents the chemical exergy. The temperature (T_o), the concentration of the environment (w_o) and pressure (P_o) can be referred to as global dead state as the system properties are expressed with '0' subscript. Only the pressure and temperature are varied related to environmental values in the restricted dead state, denoted by the '*' symbol. The exergy balance equation (8) for the control volume is given by [87]:

$$\frac{dE}{dt} = \sum\left(1 - \frac{T_0}{T}\right)Q_j + (W_{c.v} - P_0\frac{dV_{cv}}{dt}) + \sum \dot{m}_i e_i - \sum \dot{m}_e e_e - \dot{E}_D \quad (8)$$

Exergy analysis aids with the necessary parameters required to complete the design evaluation. However, it is rudimentary to investigate the exergy destruction effect of the system components on the operating costs. The thermo-economic variables are a function of thermodynamic irreversibilities and investment costs [87]. The thermo-economic model for the system's cost balancing is based on the governing equations (9.a), (9.b), and (9.c) as given by [89]:

$$\sum_{j=1}^{n}(c_j\dot{E}_j)_{k,in} + \dot{Z}_k{}^{CI} + \dot{Z}_k{}^{OM} = \sum_{j=1}^{m}(c_j\dot{E}_j)_{k,out} \quad (9.a)$$

$$\dot{Z}_k{}^{CI} = \frac{CC_L}{\tau}\frac{PEC_k}{\Sigma_k PEC_k} \quad (9.b)$$

$$\dot{Z}_k{}^{OM} = \frac{OMC_L}{\tau}\frac{PEC_k}{\Sigma_k PEC_k} \quad (9.c)$$

where τ denotes the total annual time of system operation (hours), $\dot{Z}_k$ is the capital investment cost of component k. Capital recovery factor (CRF) can be calculated from equation (10) as given by [87]:

$$CRF = \frac{i_{eff}(1 + i_{eff})^n}{(1 + i_{eff})^n - 1} \quad (10)$$

The cost rate associated with exergy loss or levelized carrying charges are determined from equation (11) as given by [87]:

$$CC_L = TRR_L - FC_L - OMC_L \quad (11)$$

Overall, it is observed that lower cost is obtained by achieving higher SWDP, PR, COP, SCP, and exergy efficiency. A similar condition can be attained by optimizing the operating components and designing the high-efficiency components.

3. Comparative analysis of ADS

Table 2 represents a summarized form of the reported literature regarding the performance parameters of various AD cycles. In addition, the unit features are also represented, such as E_a (kJ/mol), D_{so} (m^2/s), T_{source}, and the unit configuration. The table exhibits the improvement in the performance of traditional AD systems that can be made by employing different techniques such as multi-stage and multi-effect processes along with integrated ADS and similar technologies. Furthermore, as per available literature, the system performance can be improved by applying various modifications in the thermodynamic balance of the system. The key findings from Table 2 are presented here. In addition, the dynamic behavior of the adsorption chiller was studied [90] to analyze the effect of adsorbent layers and size on the performance. It has been observed that the smaller layer and grain size improve the coefficient of performance and specific cooling power of the system compared to the large layer and grain-sized adsorption chillers.

Reducing the size of silica gel and layers can increase the system size and cost, but an adsorption bed with high packing density and thermal conductivity can commercialize the chiller [90]. Therefore, a comparative study was conducted for the performance evaluation of a four-bed adsorption cooling and desalination [91]. The adsorbate pairs studied were AQSOA-Z02 + water and silica gel + water as working pairs. It was observed that silica gel is recommended for desalination, and AQSOA-Z02 is suitable for cooling. In addition, a study to analyze the performance of MED and AD hybrid systems was carried out [92]. It was concluded that hybridization improves water production by three folds.

Similarly, Wu et al. [100] carried out a thermodynamic study that concluded that lower cooling water temperature improves the system performance. The performance evaluation of solar hot water, waste heat-assisted laboratory-scale 2-bed adsorption cooling cum desalination cycle was performed [93]. It was concluded that achieving a high efficiency from an adsorption cycle produces two advantageous effects: desalting and cooling. In the AD cycle, the waste-heat recovery and conversion for utilization directly impact global warming and carbon emissions. The performance of an advanced adsorption desalination cycle was predicted and modeled [94]. A condenser–evaporator heat recovery scheme was employed, which resulted in a higher water vapor uptake than the traditional cycle, and the performance improvements are evident when plotted on a P–T–C state diagram. A remarkable improvement is observed in the specific water production capacity, which in turn increases the yield. Similarly, when low-temperature waste heat as thermal energy is used as input, the specific electricity consumption of the advanced cycle is only two times the thermodynamic limit needed for the desalination of seawater. In summary, the AD system performance can be improved by employing multi-stage and multi-effect designs, ejector integrated technology, and operation with various hybrid technologies, driven by solar energy or using low-grade waste heat.

Table 2. A quick literature review for the performance parameters of various AD systems from some of the recent studies.

Unit feature and system configuration	T_{source} (°C)	SDWP (kg/kg adsorbent/day)	SCP (TR/ton of adsorbent)	Cycle time (s)	E_a (kJ/mol)	D_{so} (m^2/s)	Schematics	Reference
ADCS employing copper sulfate, driven by low-grade heat sources. Sun-Chakraborty (S-C) and Dubinin-Astakhov (D-A) models have been used for fitting isotherms results, while the linear driving force (LDF) model has been used for the kinetics results. C= 0.51 kg/kg	25	8.2	64.54	NA	25.053	1.89×10^{-7}	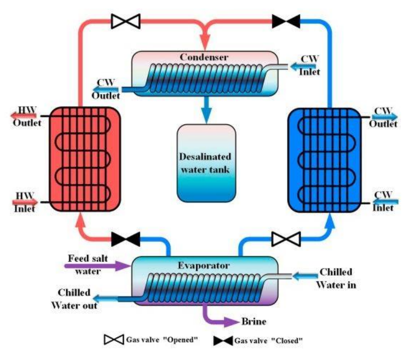	[95]

Solar-assisted adsorption (AD) cycle produces two valuable effects, namely cooling and desalination, low-temperature heat input such as thermal energy from solar collectors	7-10	3-5	25 – 35	NA	NA	NA	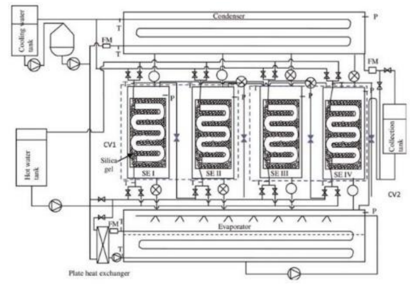	[93]
Adsorption chiller, single effect, employing two adsorbent beds with various layers of loose grain configurations and silica gel particle sizes, based on experimentally confirmed adsorption isotherms and kinetics data	80	NA	NA	NA	4.2×10^{4}	2.54×10^{-4}	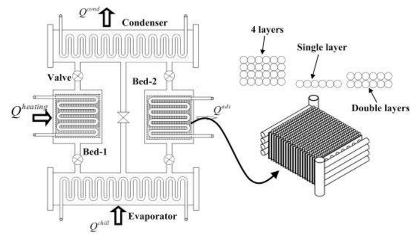	[90]
Advanced Adsorption desalination (AD) cycle with internal heat recovery between the condenser and the evaporator, investigation on the efficacy of a silica gel–water-based ADC	70	9.34	NA	600	4.2×10^{4}	2.54×10^{-4}	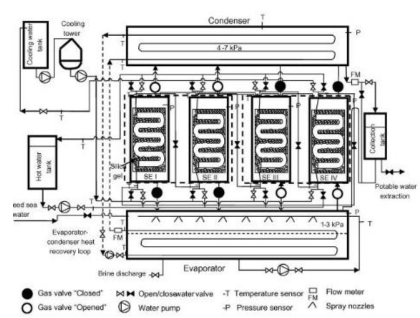	[47]
MEDAD cycle, adsorption heat pump, open cycle, Zeolite 13X as the solid vapor adsorbent	120–195	0.12	NA	NA	NA	NA	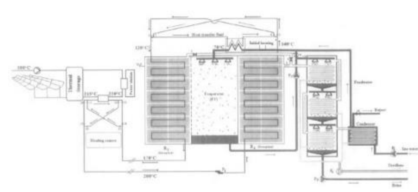	[14]

AD plant, experimental investigation presented concerning assorted primary coolant and feed conditions four beds, single-stage	85	4.7	NA	180	NA	NA	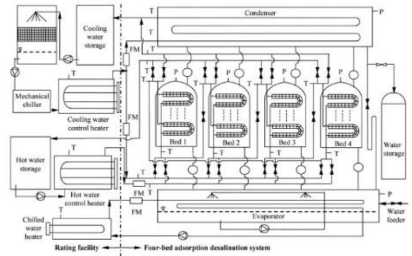	[13]
AD plant, four beds, single-stage, thermally driven cycle	84	7.8	NA	NA	NA	NA	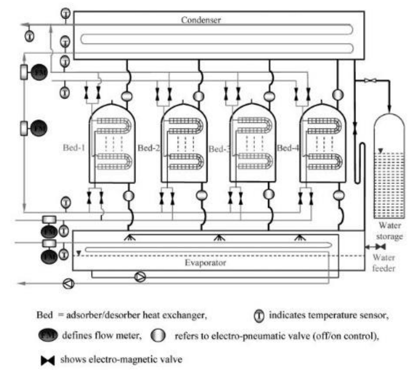	[96]
AD cycle, four beds, single-stage, waste heat-driven, employing 30°C chilled water temperature	85	8	52	960	4.2×10^{4}	2.54×10^{-4}	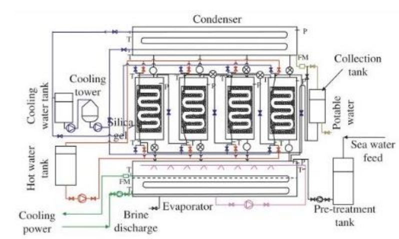	[79]
AD plant, four beds, single-stage, silica gel adsorbent	85	12.5	NA	NA	4.2×10^{-7}	2.54×10^{-4}	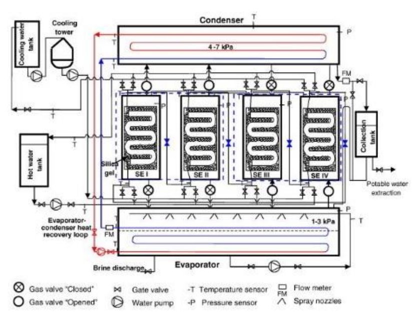	[59]
AD cycle, advanced two bed with internal heat recovery, recovering the latent heat of condenser and dumping it into the evaporative process of	85	13.46	NA	1440	NA	NA	NA	[49]

the evaporator, silica gel A++								
AD cycle, two beds with internal heat recovery and encapsulated evaporator-condenser, low-grade waste heat driven	85	26	NA	600	4.2×10^{-7}	2.54×10^{-4}	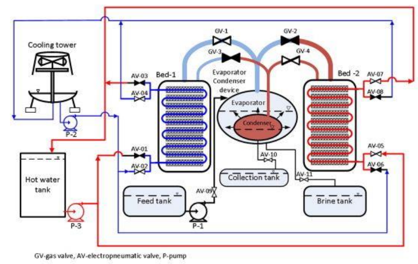	[94]
MEDAD cycle, vapor uptake by the adsorbent in AD cycle, extracting from the vapor emanating from the last effect of MED, two beds, 10 kg of silica gel	50	5	NA	NA	4.2×10^{-7}	2.54×10^{-4}	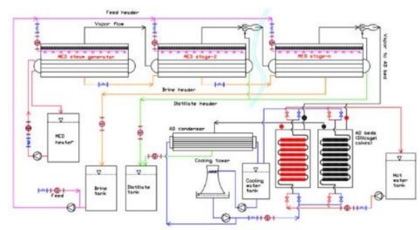	[92]
AD system incorporates transient heat and mass transfer processes in the stream-wise direction of the adsorbent bed, two beds, silica gel	80	0.315	NA	NA	42	2.54×10^{-4}	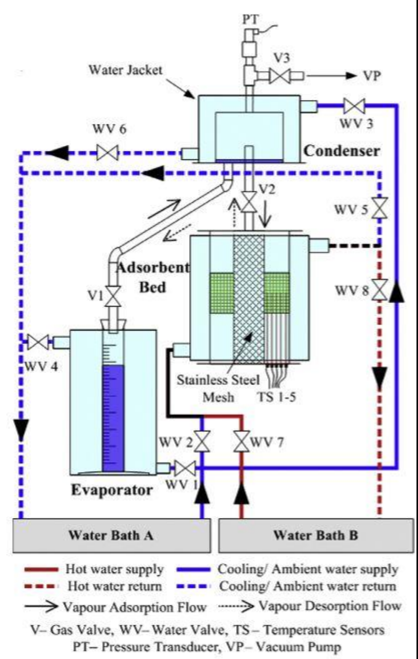	[97]

AD cycle, investigation of condenser evaporator on cycle performance, two beds, T_{evap} = 30°C, T_{cond} = 10°C	85	10	77	425	NA	NA	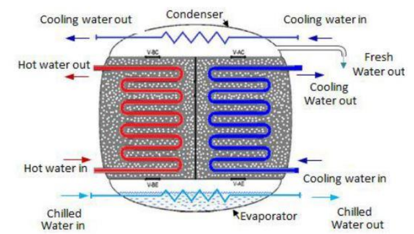	[98]
AD cycle, two adsorbents; silica-gel and AQSOA-Z02 (advanced zeolite) T_{evap1} = 10°C T_{evap2} = 30°C	85	6.2	53.7	600	4.2× 10^4	2.54 × 10^{-4}	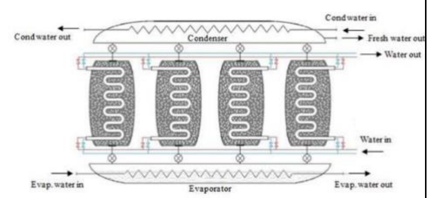	[91]
		7.2	55					
MVC-AD system investigation, two beds, single-stage, a mathematical model has been designed to simulate the operating of the proposed system	NA	14	59.71	NA	41.94	2.54 × 10^{-4}	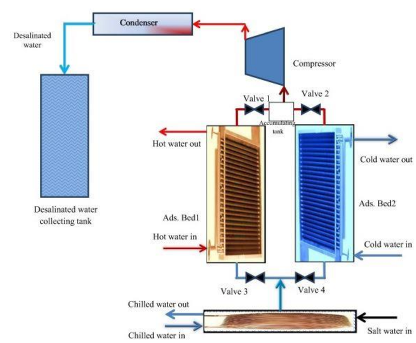	[36]
AD cycle, two-stage, two bed, an attempt to model the inter-stage pressure dynamics, P_{evap}=1.7 kPa, silica gel RD adsorbent	85	0.9	6.8	3800	NA	NA	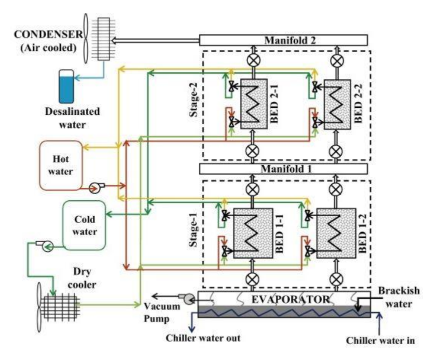	[99]

Solar adsorption desalination-cooling (ADC) system, adsorption characteristics of the silica gel-water pair are evaluated, a theoretical dynamic model is developed to predict the system performance, single-stage	95-75	4	33	650	0.51597	2.54 × 10^{-10}	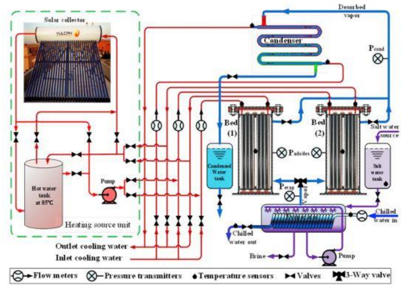	[100]
AD system, thermodynamic performance evaluation, MOFs suitability assessment for AD, CPO-27 (Ni), single-stage	150	4.3	35.3	700	0.45	NA	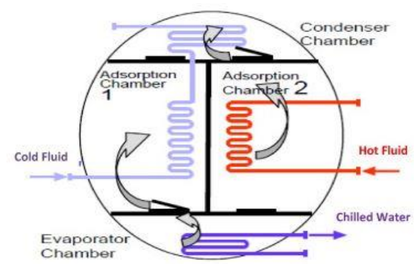	[101]
AD system, thermodynamic performance evaluation, MOFs suitability assessment for AD, aluminum fumarate, single-stage	150	6.5	22	700	0.324	NA	NA	[101]
AD system, numerical and experimental investigation of CPO-27(Ni) employment, one bed at T_{cond} = 5°C and T_{evap}= 40°C,	95	22.8	65	600	0.648	NA	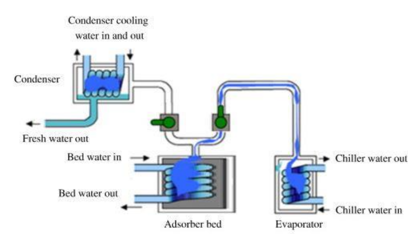	[102]

ADEJ-HR cycle, ejector integrated, single cycle to increase the productivity of desalinated water, heat recovery between the condenser and the evaporator	95	40	65	800	32	NA	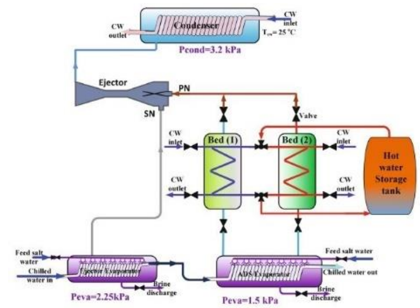	[103]
AD system, a thermodynamic mathematical model was derived and evaluated by valid experimental data, heat and mass recovery, two bed, single-stage	95	16 - 40	NA	600	0.756	2.54 × 10^{-4}	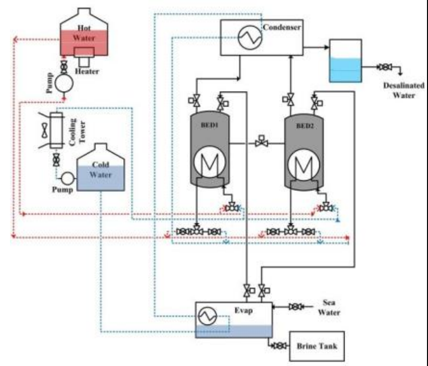	[40]
Novel hybrid AD-(water-heated) HDH system, low-grade energy source, investigation of freshwater and cooling capacity, silica gel adsorbent	< 85	9.6	24 - 25	NA	42	2.54 × 10^{-4}	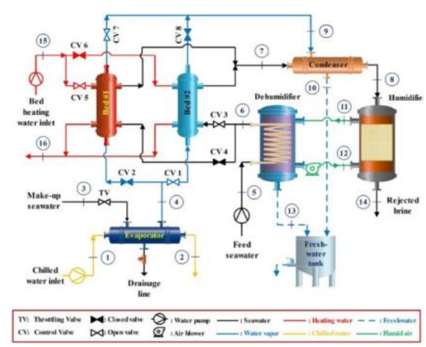	[104]

Key: NA: not available.

4. Adsorption desalination (AD) technologies

The conventional ADS was developed in 1984 by Broughton [33] derived from adsorption chillers [105–108]. Earlier, freshwater was used as a refrigerant [55]. However, it gives low system performance in terms of COP, cooling capacity [77] with large energy consumption [59]. Therefore, the system performance evaluation, along with several modifications, has been presented in the literature. In this regard, various studies have been reported to improve the system performance using appropriate adsorbents with promising adsorption capacity and kinetics [77].

Various configurations of adsorption desalination cycles are presented in the literature, which are listed in Fig. 7. Similarly, a two-stage ejector ADS cycle was proposed [109] to achieve high efficiency and water production. Hybridization between the AD cycle and two ejectors was reported along with silica gel-water as an allowing pair to increase the significant productivity. The hybrid cycle consists of a pair of condensers, evaporators, ejectors, and sorption beds. The adsorption desalination/2 ejectors system (AD2EJ) was based on COP and SDWP, where mathematical models for ADS cycle and ejectors are validated. At a regeneration temperature of 85°C and the optimal half-cycle time of ~400s, it was observed from the numerical analysis that the SDWP and COP are found to be 23.0 m^3 per ton of silica gel and 1.64, respectively. Thus, the freshwater production from AD2EJ is three times higher than conventional AD systems. The system is further enhanced by connecting the evaporator condenser through an internal heat recovery circuit. The coming subheading will discuss various AD techniques/configurations accordingly in detail.

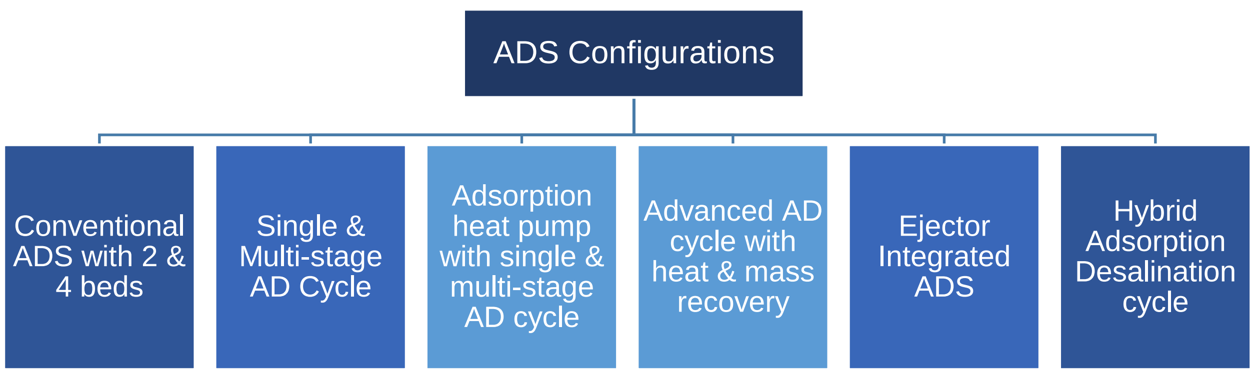

Fig. 7. Categorization of adsorption desalination system configurations based on the mode of operation.

4.1.Ejector integrated ADS

A concept of ejector integration with the adsorption desalination cycle has been reported [103]. The concept aimed to increase the productivity and COP of desalinated water. The significant design improvisation was based on ejector installation after the adsorption bed, which was to be driven by desorbed vapor. The desalination productivity of the cycle was increased by connecting the evaporator to the secondary ejector nozzle for vapor extraction [103]. The ejector increases the pressure of secondary vapor, bypassing the primary vapor through a converging-diverging nozzle. Due to the difference in velocity of secondary and primary flows, the flows do not get mixed until the sonic velocity of secondary flow is reached [110].

An innovative ADEJ cycle is expressed, as shown in Fig. 8 [103]. The presented study involved the simulation of ADEJ under constraints of uniform pressure and temperatures. Previous literature has reported the validation and use of the lumped parameters model in multiple studies [59,95,111].

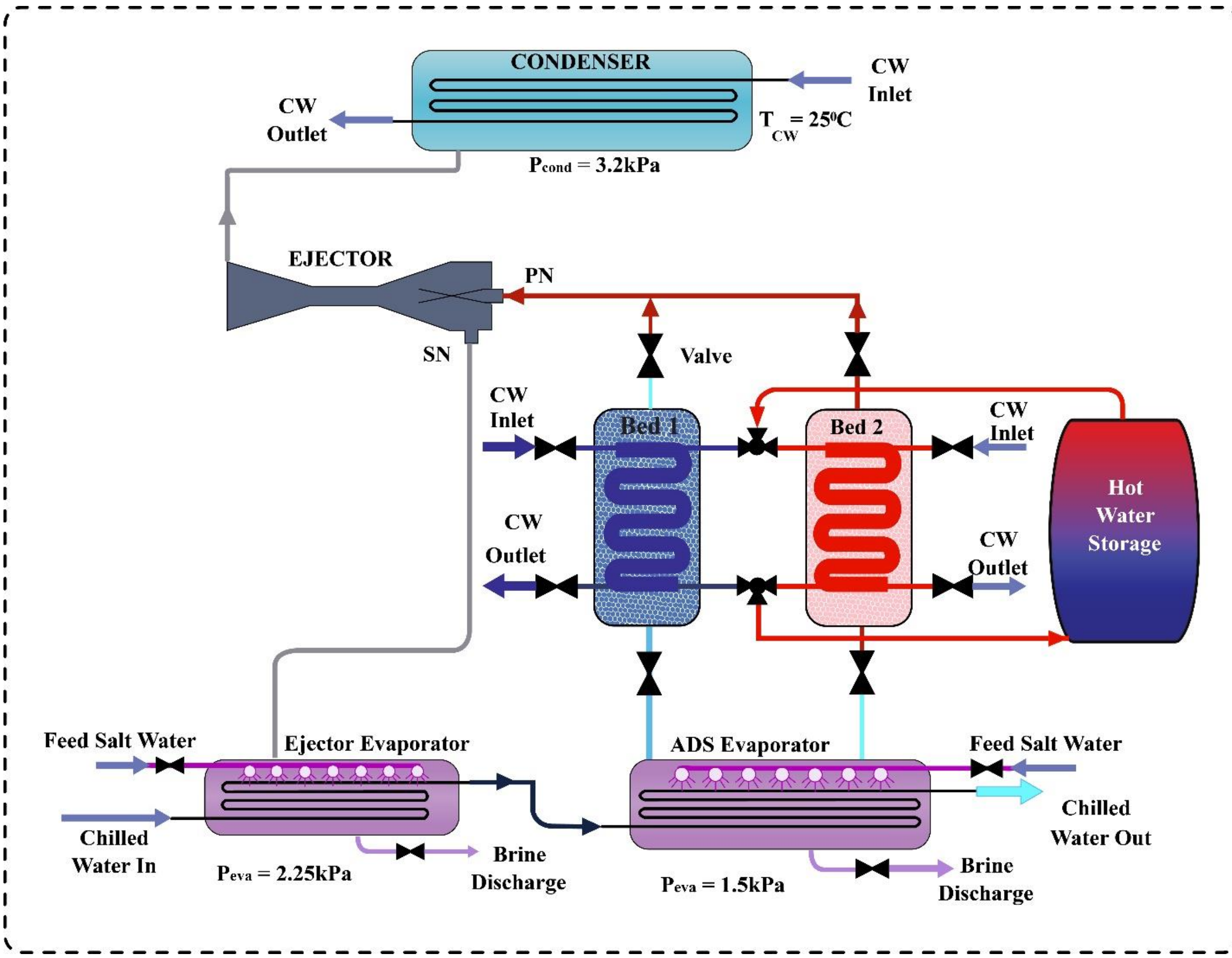

Fig. 8. Schematic diagram of integrated ejector adsorption desalination cycle, reproduced from [103].

The study [103] analyzed the effect of an integrated ejector on ADS with condenser/evaporator heat recovery. The governing mass and energy balance for ADEJ is presented by equations (12) and (13) as given by [103]:

$$\left[\frac{dM_{SW,evap}}{dt}\right]_{Ejectorevap} = \left[\theta\left(m_{\dot{S}W,in} - \gamma m_{\dot{b}} - n.ER\left(\frac{dC_{ADS}}{dt}\right)M_{sg}\right)\right]_{Ejectorevap} \quad (12)$$

$$\left[M_{SW,evap}\,, \frac{dX_{SW,evap}}{dt}\right]_{Ejectorevap} = \left[\theta X_{SW,in} m_{\dot{S}W,in} - \gamma X_{SW,in} m_{\dot{b}} - n.ER.X_D\left(\frac{dC_{ADS}}{dt}\right)M_{sg}\right]_{Ejectorevap} \quad (13)$$

where n, r, and ϴ are switching operating modes [59]. ER is the ejector entrainment ratio equal to the secondary fluidness flow rate to the primary fluid mass flow rate. The regeneration temperature has an insignificant effect on the ejector entrainment ratio and ejector compression ratio. The average ER and CR were about 0.5 and 1.42, respectively. Therefore, many studies investigated the vapor compression cycle (VCC) to benefit the kinetic energy available to improve the cycle COP. In a vapor-vapor ejector refrigeration cycle, the ejector functions similar to a compressor. As inlet secondary vapor passes through a converging-diverging nozzle, the pressure is increased by the ejector [59].

A study had been carried out which investigated the integrated ejector within the vapor compression cycle. The study was primarily focused on testing the effect of condensing, generating, and evaporating temperatures of the ejector sub-cycle on the ejector vapor compression cycle. Another study [112] proposed an ejector with hybrid VCC, which reported that EVCC performance largely depends on the ESC temperatures. Nevertheless, there is a similarity in the variation of the degree of sub-cooling at the vapor compression sub-cycle (VCSC) to improvement in COP at ejector vapor compression cycle over vapor compression sub-cycle. Further, it was observed that the system under certain operating conditions yields a comparatively more significant COP improvement of about 15.9-21.0%.

A hybrid vapor compression refrigeration system (HVCR), which consists of a combined ejector refrigeration (ER) system and vapor compression refrigeration system (VCR), was simulated [113]. It was found that the ejector and gas cooler accounted for a large percentage of total exergy destruction. Therefore, the HVCR system expressed an improved COP by 25% than the conventional VCR system. Furthermore, an adsorption refrigeration system was proposed [114]. The system utilized two ejectors as the cycle power source in the place of mechanical pumps. The location of the liquid-vapor ejector is at the absorber inlet. It has been concluded that the novel combined double ejector refrigeration cycle (DEARC) when compared with the conventional air-cooled absorption refrigeration cycle, which sacrifices a portion of refrigerant, leads to a decreased COP. Notwithstanding this, a maximum COP of ~0.63 can be reached which encourages the modification and practical use under exhaust heat conditions.

A simple ejector without moving parts combined with a solar-assisted absorption cooling system employing LiBr/H_2O as a working fluid was studied. The system performance evaluation was expressed [115]. As a result, it was observed that the post addition of the condenser along with condenser and evaporator load is found to be perpetually increased as compared to the primary cycle, which suggests that the increase in the system's cooling capacity is due to the increase in entrainment ratio and the evaporator temperature. A 60% increase of COP of the modified cycle was witnessed to that of the primary cycle at the same temperature and pressure. Adopting this process enhances the functions, stabilizes the refrigeration system, and qualifies the system to work under the raised temperature of the condenser. A combined ejector integrated system is believed to work efficiently with other systems and increases the COP. The main goals are the maximization of AD system performance by ejector integration before condenser in an ADS technology. Simulation, experimental and theoretical scenarios contribute to paving the way for researchers to industrialize AD systems. Furthermore, the ADEJ system using energy and mass balance ejector-integration strategy can improve the system performance.

4.2.Integrated evaporator-condenser cascaded ADS

An AD plant layout was developed and evaluated using numerical simulation [48,49]. The AD cycle suggested in Fig. 9. uses internal heat recovery and heat transfer between the encapsulated condenser and evaporator. Shell-and-tube heat exchangers are used in the integrated evaporator–condenser unit. One of the benefits of this integration is the employment of working fluid circuits to heat the evaporator and cool the condenser, which leads to a considerable reduction in the cost of pumping power. This arrangement also reduces the resistances of heat transfer and increases seawater evaporation rates. Theoretical findings showed that this advanced arrangement could produce an SDWP of 26 kg/kg of silica gel per day utilizing a hot water temperature of 85 °C, twice as high as the primary plant. Furthermore, the performance of other configurations, comparable to the current pilot adsorption desalination plant at NUS, was statistically investigated. This alternate configuration with internal heat recovery is an entirely integrated condenser–evaporator system that employs a cooling fluid circuit to provide the condenser's condensation heat to the evaporator [116].

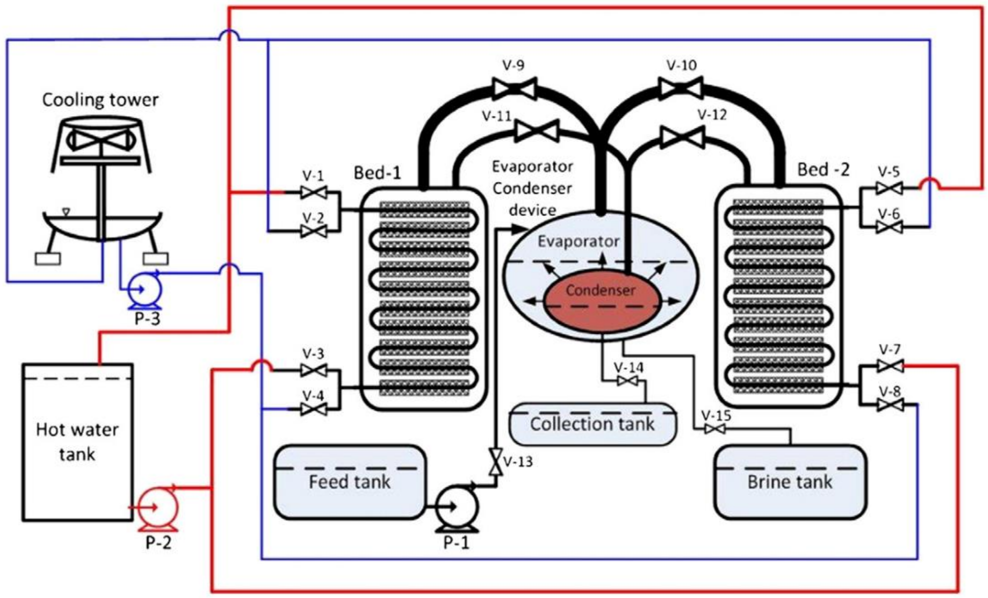

Fig. 9. Schematic diagram of AD cycle with an integrated evaporator-condenser unit, [59].

Integrating the condenser-evaporator, both coolant circuits for essential cycle operation are omitted, resulting in considerable savings in pumping costs. Instead, heat is transmitted directly through the walls of the condenser tubes within the evaporator shell. As a result, the device's heat transfer resistances are decreased, which improves the film evaporation of water vapor from seawater. In addition, a benefit of combining the condenser-evaporator unit is that the evaporator has a more significant vapor pressure. Therefore, it significantly enhances the rate of silica gel vapor absorption over the specified adsorption process. The benefits of the advanced AD cycle design, i.e., an integrated condenser-evaporator [59] are: (i) a decrease in parasitic electrical power as a result of the exclusion of pumps from the chilled and cooling water circuits, (ii) the pressurization effect improves the silica gel's adsorption capacity, (iii) the effective condensation temperature in the condenser is lowered, which facilitates desorption, and (iv) the heat source temperature is lowered to 50°C for the AD cycle.

Several studies have further investigated the condenser-evaporator integrated unit. The unit was explained by Thu et al. [47,49] for various heat recovery designs of ADS on 2 or 4-bed modes. The integrated evaporator-condenser was further analyzed for the effective mass of ADS with heat recovery to obtain the desired results. The evaporator's temperature is raised to ensure condenser heat recovery, leading to an increase in water production. This amount later improved thrice than the conventional ADS [15,46,117]. A study was carried out as the comparative analysis of integrated evaporator-condenser and conventional adsorption desalination system. The newly developed system's cycle design consisted of four beds, including a condenser, evaporator, and one integrated evaporator-condenser unit. The cycle is composed of two single-stage regular ADC. The new multi-cycle configuration benefits from reducing condenser temperature, increasing the quantity of desalinated water and generating cooling power at the reduced evaporator temperature. Consequently, the integration of heat and mass aids ADC performance improvement.

4.3.Solar/sunlight regenerable ADS

Waste heat and solar energy can be efficiently used to run the adsorption desalination cooling system (ADCS) [118]. A 4-bed single-stage solar-driven ADS was developed and analyzed for system dynamics [119]. The system consisted of a non-concentrating solar collector providing low-grade heat, utilized by the thermal desalination cum refrigeration cycle. It was designed to generate cooling and desalinated water when combined thermal compression and flash evaporation are employed. It is observed that a system cooling and desalination capacities are affected with solar energy utilization simultaneously. The condenser temperature rises with the the increase in operating pressure ratio which rapidly degrades the system performance. Consequently, two-stage ADS can be employed which aids in improving system performance.

A detailed thermodynamic analysis of the solar-based adsorption desalination and cooling system was performed as shown in Fig. 10 [120]. The system utilizes the low-grade heat from the solar collector to drive the system. The thermal compression and combined flash were employed for the production of cooling and potable water. The findings indicate that the hot water intake temperature, cooling water temperature, and condenser temperature all significantly influence the system's water output, energy consumption, and COP. Low cooling water temperature, low condensation temperature, and high hot water intake temperature result in improved system performance. The rate of water production increases as the temperature of the hot water intake rises, eventually flattening off at higher temperatures. This rising trend of water output with temperature is caused by an improvement in the amount of water desorbed from the adsorbent as the hot water temperature rises.

The performance evaluation of solar-driven AD cooling system was conducted [100]. The system was tested with 13.5 kg of commercially available silica gel. The working pair of silica gel-water was evaluated and the system performance prediction was made based on theoretical dynamic model. The system resulted in COP, average specific daily water production, the average specific cooling power of 0.45, 4 m^3 per ton of silica gel, and 112 W/kg, respectively. A study on the water quality analysis of the solar-driven adsorption desalination cycle was presented [121]. A significant reduction in TDS levels of feed seawater from approximately 40,000 ppm to less than 10 ppm is evidence of process efficiency. In the desalinated water, there are deficient levels of chloride, magnesium, sulfate, silicate, sodium, calcium, and bromide, even less than 0.1 ppm. The conductivity parameters of product water were composed of the distilled water conductivity levels ranging between 2 and 6 μS/cm.

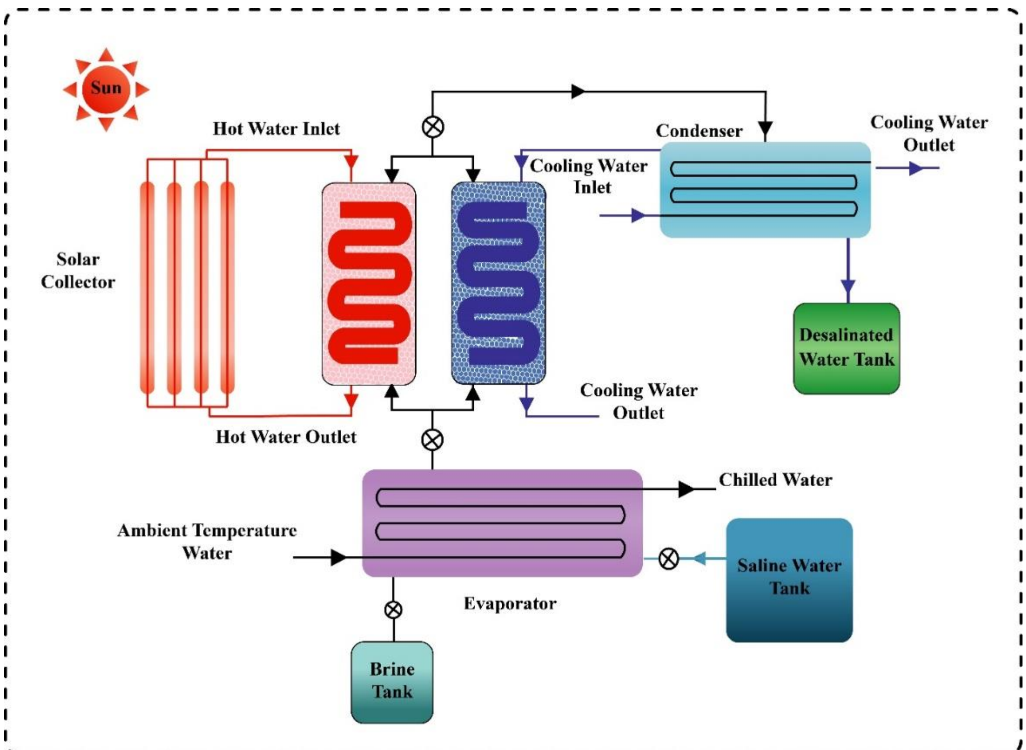

Fig. 10. Schematic diagram of a solar-driven adsorption desalination system, reproduced from [120].

The performance investigation of the solar-driven dual effect adsorption cycle for the production of potable water and cooling effect was performed by Ng et al. [93]. It is driven at low-temperature heat, such as thermal energy provided by solar collectors. Mathematical modeling of the system was discussed along with key parameters based on SCC and SDWP. The system uses a flat plate type solar collector and silica gel-water based adsorption desalination cycle. The system experimentation exhibit capacity of chilled water production at a temperature and SCC range variation of 7-10°C and 25-35 Rton/tonne of silica gel, respectively. Consequently, the adsorption desalination cycle possesses a conversion or performance ratio of 0.8-1.1 and daily production capacity, SDWP of 3-5 m^3 per tonne of silica gel per day. Similarly, a solar-assisted adsorption refrigerator was developed [122]. The system performance can be improved by well-insulating the cold chamber and using automatic valves, potentially improving efficiency. A numerical and experimental investigation was carried out by Ahmadi et al. [123]. The feasibility investigation of the solar eductor-assisted desalination system performed resulted in a promising performance of the closed educator installed at the exterior of the evaporation chamber. It was revealed from the experimental analysis that reducing the flow rate of water can reduce energy requirements. A thermodynamic framework was presented by the authors [7] to address energy efficacy. It was observed that there is 2.5-3% energy consumption by the thermally driven system when integrated with power plants. Furthermore, it must have innovative systems to fulfill the 20-30% thermodynamic limit by 2030.

Desalination technology is extensively employed for the reduction of escalating water scarcity. Currently, membrane and thermal-based desalination technologies are used to address the issue and freshwater production. Nevertheless, thermal technologies' energy consumption is relatively high. For example, multi-effect and multistage desalination have an energy consumption of 14-27 kWh/m^3. The drawbacks of membrane-based techniques include the chemical consumption in dechlorination & cleaning and relatively high energy consumption of 1.6-6 kW/h^3 [124–126]. Similarly, efficient salt removal can be conducted by passing brackish water from the adsorbent or ion-exchangers-filled columns [127]. Mainly, in the water industry, there is an implementation of thermo-responsive ion adsorbent-based desalination. The process of ion-adsorption is energy efficient, but for regeneration, the requirement of thermal energy at increased temperature (i.e., 80°C) is substantial [126,128–130].

4.4.Multi-effect ADS

A parallel feed MED and AD system integrated is usually employed to replicate the process. The schematic diagram is shown in Fig. 11 [92]. The details of the AD cycle function can be studied from the literature [41]. In another study [92], the suggested simulation model by the authors for the MED system, horizontal tubes falling film evaporators are employed. The feed is de-aerated to eliminate the oxygen (through a de-aeration tank with a vacuum pump) before being fed parallel to all evaporators—built-in pre-heaters route feed-in evaporators before being sprayed onto a tube bundle through spray nozzles. The first stage, often known as the steam generator, is utilized to generate initial steam. The hot water is cycled via the tubes, and pressure is controlled to evaporate the seawater at the appropriate temperature, corresponding to the hot water temperature. The vapors generated are then allowed to move to the tube side of the subsequent effect. Condensation heat is utilized to vaporize the feed sprayed at that step. Similarly, vapors are cascaded in subsequent phases until the final effect is achieved (nth effect). Intermediate steam jet ejectors are supplied to remove non-condensed vapors from each stage distillate box. The final stage of MED is linked to AD beds to adsorb the vapors onto adsorbent (silica gel) packaged in the shape of cakes. Because of the strong affinity of the adsorbent for water vapors, this combination of MED and AD lowers the temperature of the last stages below ambient, allowing for more stages and higher recoveries while also reducing the possibilities of corrosion. The vapors are desorbed and condensed in the condenser with the help of the heat source. A vacuum pump is introduced to keep the pressure level in the MED stages and the AD machine constant. It also aids in removing air that has entered the system as a result of a leak. A distillate collecting tank is supplied to collect distillate across all stages of the MED and the AD condenser.

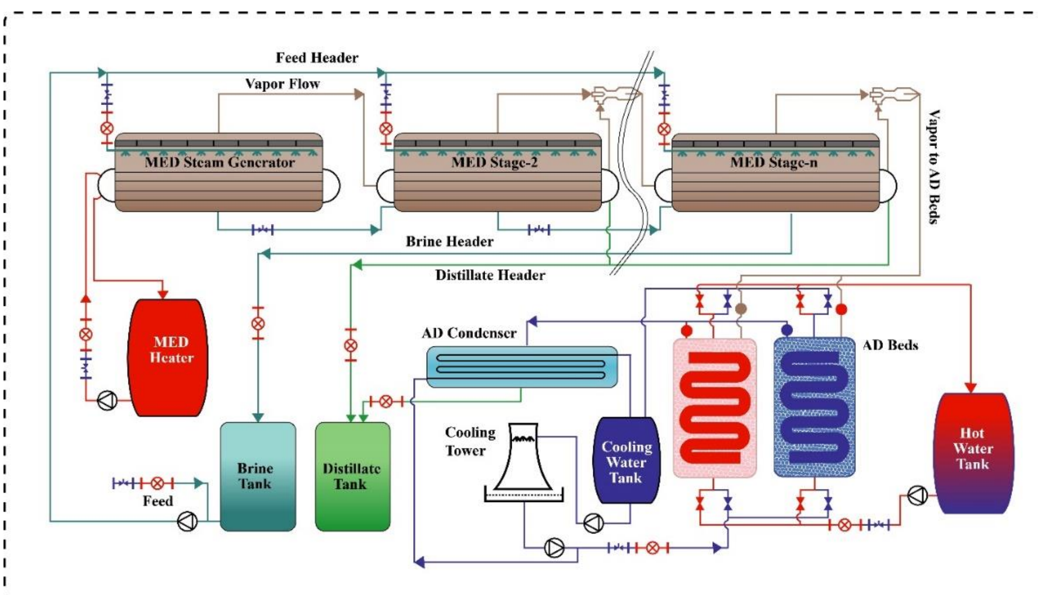

Fig. 11. Schematic representation of Multi-Effect Adsorption Desalination System (MEDAD), reproduced from [92].

The thermodynamic synergy can hybridize the emerging adsorption desalination systems and the conventional ADS for their thermodynamic synergy. The authors carried out a similar hybridization of conventional multi-effect distillation (MED) with an emerging low-energy adsorption cycle, which resulted in an advanced desalination cycle [92]. As the adsorbent uptakes the vapor, it yields the cycle integration and extraction from the vapor emanating from the last effect of MED. Additional evaporation-condensation stages can be accommodated by the system as the temperature difference range is increased. The study presented the numerical model of the proposed MEDAD cycle, which comprises the water production rate of the conventional MED cycle. The hybridized MED scavenges heat from the ambient air and allows the latter stages of MED to operate at a lesser temperature than the ambient air. The latter stages' reduced saturation temperatures eradicate the fouling and scaling effects, but improved water recovery from feed seawater may increase solution concentration. Similarly, a study on efficiency examination was carried out by the authors [131]. A MED system was investigated, and it was found that seawater thermocline (ST)-driven MED system can increase the system efficiency 2 folds and be regarded as the most appropriate ‘green desalination’ method.

Some studies were also reported on the thermo-economic analysis of MED systems by employing exergy analysis and optimization methods [132–137]. In addition, various heat performance pump coupled MED systems were also studied by researchers [138,139]. For example, an integrated adsorption vapor compression (ADVC) system was proposed [140]. The system employs the vapor obtained from the last stage of MED for adsorption, whereas, from desorption, the regenerated water vapor is forwarded to the first effect of the MED cycle. Consequently, the MED system condenser is eliminated in the combined cycle, and the performance ratio is improved to two folds [141–144]. Notwithstanding this, some other research on similar technologies, such as vacuum multi-effect membrane distillation technology, was investigated by Chen et al. [145].

A hybrid MEDAD cycle was analyzed by the authors [146]. The system's hybridization allows the conventional MED cycle to be operated at a low temperature of 5°C. As a result, the MEDAD cycle resulted in a significant increase in distillate production as the MED can scavenge the ambient energy whereas, the conventional AD cycle is driven by low-temperature waste heat obtained from renewable or exhaust sources. The study's experimental setup consisted of MEDAD and 3-stage MED plants, assorted and tested at 15°C-17°C temperature from a waste heat source. An in-depth observation and monitoring of the system result in the MEDAD cycle's synergetic matching lead to a significant increase in distillate production of about 2.5-3 times compared to the conventional MED cycle.

A hybrid MEDAD cycle was developed [173], as shown in Fig. 11, operating at sub-atmospheric temperatures and pressures. A quantum performance enhancement has resulted from the hybridization of the multi-effect distillation and adsorption desalination cycle. The symbiotic enhancement resulted in brine heater usage emanated waste heat, which cascaded the adsorbent's regeneration temperature. Furthermore, the decreased saturation temperature of 5°C was provided by vapor extraction from the last MED stage by AD cycle, resulting in scavenging of heat leaks into the MED stages from the ambient. The hybrid desalination system augments the desalination plant's capacity for water production twice. A simulation of the 8-stage MED cycle was used for the demonstration of a hybrid cycle. The silica gel's sorption properties were employed as a mechanical vapor compressor to reduce the saturation temperatures of MED stages. The kinetics of adsorbent-adsorbate such as silica gel-water and adsorption isotherm were employed for modeling energy, mass, and concentration equations. The MEDAD cycle was operated at 65°C-90°C temperatures, and upon comparison with conventional MED, the cycle exhibited an augmented water production rate from 60% to two folds and an increase in GOR and RP by 40%.

4.5.Hybrid ADS

In recent years, various studies have been conducted to address the limitations of conventional ADS by designing some improved designs [147]. The conventional ADS works at a relatively low temperature where evaporation occurs in the ambient, typically around 5°C to 20°C [72]. Solar heating was employed to desorb the water vapor, which condenses at high altitudes and produces pure water without any supply of carbon-based energy. Furthermore, theoretical analysis was performed on a low-grade solar heat-driven water desalination system [11]. The system possessed distinction from conventional ADS as natural forces create vacuum conditions incorporated into a single design consisting of an evaporator, condenser, solar heating systems, and injection. The numerical simulations of the system resulted in 90% or higher efficiency. The simulation for a solar-driven adsorption desalination system was performed [14]. The theoretical model combined with an adsorption heat pump using zeolite was analyzed to determine the system energy consumption and water production. A solar-driven dual effect adsorption cycle was studied by Ng et al. [93]. The solar AD cycle's performance investigation resulted in desalination and cooling at low-temperature heat input, i.e., thermal energy from solar collectors. Further mathematical and experimental modeling resulted in a performance ratio of 0.8-1.1 with producing SDWP of 3-5 m^3 per tonne of silica gel per day at a temperature of 7-10 °C. Consequently, a low-grade heat-driven adsorbent cycle integrated with membrane processes can ensure 150% of chemical rejection and ensure about 99% energy-saving [148]. Furthermore, as renewable energies are environment friendly having no negative impact, the desalination systems are driven by renewable technologies to ensure the future sustainability of water supplies [149].

An innovative pressure swing adsorption cycle (PSAD) was proposed by the authors [150], which employs a thermal vapor compressor for steam regeneration. The study revealed that primary steam having 2 bar of pressure can generate a compression ratio of 3-4. Consequently, the desalination cycle can be operated by re-utilizing the discharged steam, hence maximizing the exergy of steam. Several other studies were performed for the analysis of AD cycle at different regeneration temperatures examining the operational strategy, theoretical model, numerical simulation, and performances at different heat source temperatures [151][152] [44]. Consequently, a similar study was also reported [153]. To analyze the performance of desalination and cooling systems concerning time, a study investigated two-half cycle ADS [154]. The effect of time variation by changing the interval of adsorption-desorption by 200s to 700s and switching interval of 20-40s. At cooling water inlet, chilled water inlet and hot water temperature of 35°C, 7°C, and 85°C, respectively. The analysis resulted in the SCP, SDWP as 25TR, and 12 m^3 per ton of silica gel, respectively. A silica gel-water, 4-bed adsorption desalination system was studied [119]. The performance evaluation of various condenser temperatures and cycle time was carried out for the determination of optimum requirements for desalination and cooling. The simulations pointed out that the time range of the single-stage adsorption desalination system has an optimum half-cycle time of 600 to 900s to increase the cooling and desalination capacity. Therefore, as the cycle time is increased, the coefficient of performance is raised.

The studies discussed have shown the performance of silica gel as an adsorbent that can be utilized in the low heat-driven ADS, usually at a temperature of 85 °C. Various researches were conducted by Kim et al. [95] to evaluate ferroaluiminophosphate adsorbent for its potential use in ADS. FAM-Z01 possesses an equilibrium adsorption capacity 5 times higher than the silica gel adsorbent at a temperature of 40 °C. The performance of the adsorption desalination cooling cycle and the subsequent effect of evaporator-condenser temperature were mathematically studied. Further investigation revealed that when the condenser temperature is 30 °C, and the water inlet temperature is 10 °C, the system results in SCP and SDWP as 77 TR per ton silica gel and 10 m^3 per ton of silica gel, respectively.

5. Economic aspects

The advanced and conventional adsorption desalination plants of different capacities/ flow rates were analyzed for water production cost as a function of the mass of adsorbent, as shown in Fig. 12 [155]. It has been observed that the unit production cost of a conventional adsorption desalination system is nearly four times higher (i.e., ~\$1.91/m^3) than the advanced cycle (i.e., ~\$0.457/m^3). Factors affecting the unit cost of the AD system are (i) reduction in pumping power, (ii) design improvement, and (iii) improvement in the overall heat transfer coefficient of condenser-evaporator integrated design. An AD plant of 1000 m^3/day capacity has the unit production cost (operational cost+capital cost) of \$0.457/$m^{3,}$ as shown in Fig. 13. The upscaling of AD plants causes a reduction in capital cost [155]. The specific energy consumption and the energy cost of water production of the AD cycle are compared with other conventional methods such as RO, MSF, and MED [96]. The MSF cycle shows the highest energy cost of water production (i.e., US \$0.647 per m^3), whereas the AD cycle gives the lowest energy consumption of about 1.5 kW/m^3, which is equivalent to the production cost US \$0.227 per m^3. It has been concluded that the AD technology can desalinate the high salinity feed water and produce low salinity water at a low cost, i.e., US \$0.2/m^3 [96].

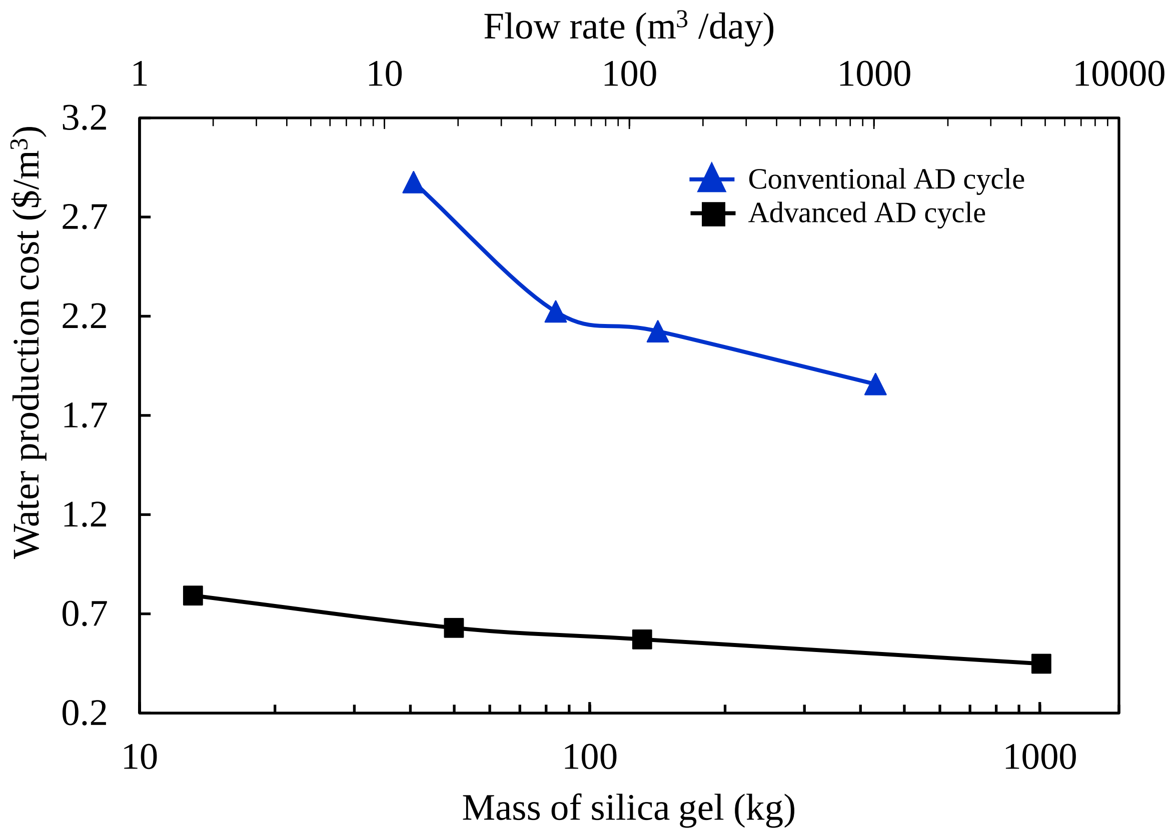

Fig. 12. Relationship between the cost of water production and the mass of silica gel reproduced from [155].

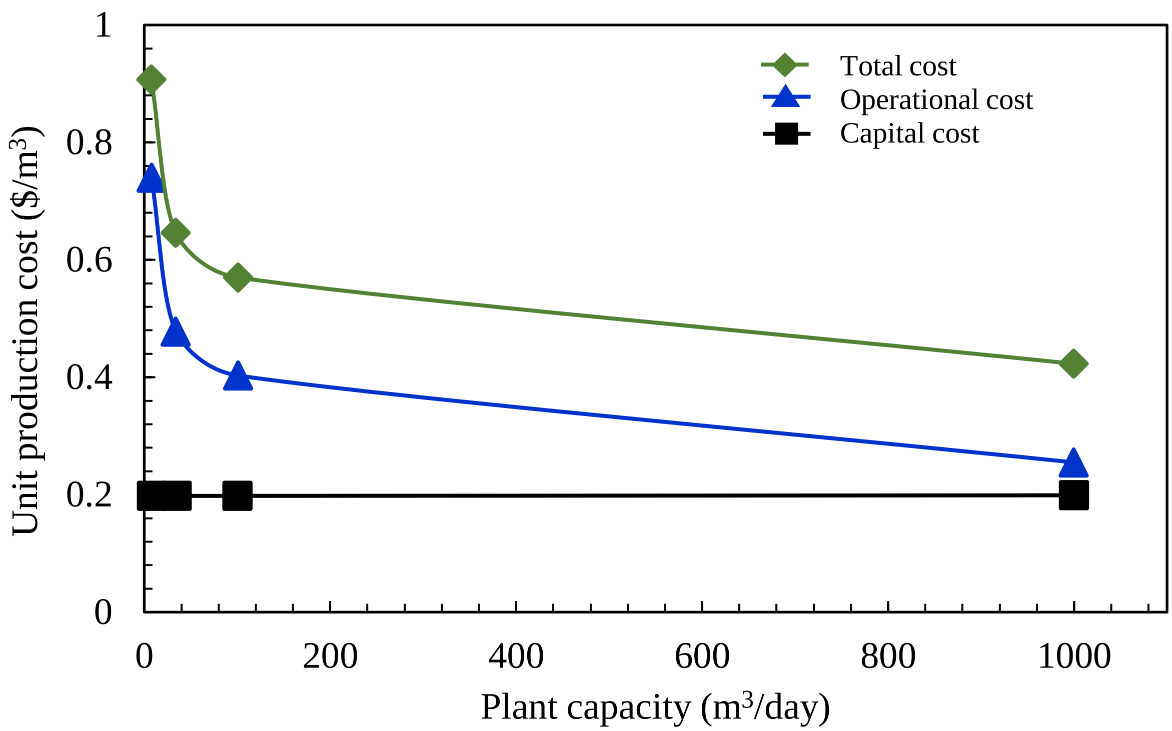

Fig. 13. The relationship between the unit production cost and plant capacity of an AD plant, reproduced from [155].

6. Conclusions

Adsorption desalination (AD) is a emerging technique for obtaining potable water from an unlimited supply of brackish water. This study discusses adsorption desalination (AD) systems and subsequent hybridization options. The AD systems are reviewed for energy consumption, water productivity, and associated performance parameters. The AD system performance has been improved with the integration of multi-effect AD designs (MED), ejector integrated technology, evaporator-condenser cascaded technology, solar and hybrid options. For instance, a combined ejector technology can stabilize the refrigeration system and increase the COP of the desalination plant. Similarly, the evaporator-condenser AD systems reduce condenser temperature, increase desalinated water production, and generate cooling power. The specific energy consumption of ADS is <1.5 kWh/m^3. For solar AD systems, the specific cooling capacity is 112 W/kg, and the COP is 0.45. The SDWP was observed as 66% for a heat and mass recovery process of 2-bed ADS. The cost of an advanced AD cycle is ~$0.457/m^3 which is four times less than a conventional AD cycle. Compared to standard MED plants, the hybridization of MED+AD improves output more than 3 times with the same TBT. The AD cost is still a challenge which can be improved with the further development and research for SDWP enhancement at low heat source temperature. The AD is emerging as a viable and realistic option for relieving global thirst and thereby going to be accessible in the global market.

CRediT authorship contribution statement

Nadia Riaz: Conceptualization, Methodology, Software, Formal analysis, Investigation, Writing - Original Draft. **Muhammad Sultan:** Conceptualization, Methodology, Validation, Resources, Writing - Original Draft, Visualization, Supervision, Project administration, Funding acquisition. **Takahiko Miyazaki:** Validation, Resources, Writing - Review & Editing, Supervision, Project administration, Funding acquisition. **Muhammad W. Shahzad:** Formal analysis, Software, Writing - Review & Editing, Visualization. **Muhammad Farooq:** Data Curation, Writing - Review & Editing, Visualization. **Uzair Sajjad:** Writing - Review & Editing, Visualization. **Yasir Niaz:** Writing - Review & Editing, Visualization.

Declaration of Competing Interest

The authors declare that they have no known competing financial interests or personal relationships that could have appeared to influence the work reported in this paper.

Acknowledgments

This research was carried out in the Department of Agricultural Engineering, Bahauddin Zakariya University, Multan-Pakistan, with the financial support of the BZU Director ORIC Grant (2020-2021) awarded to Principal Investigator Dr. Muhammad Sultan.

Appendix A

Table A1. Mathematical expressions for the classification of adsorption isotherms [156].

Classification	Name of the model	Equation of the model	Reference
Empirical adsorption isotherm models	Linear isotherm model (Henry's law)	$q_e = KC_e$	[156]
	Freundlich isotherm	$q_e = K_F {C_e}^{1/n}$	[157]

	model		
	Redliche-Peterson (Re-P) isotherm model	$q_e = \frac{K_{RP}C_e}{1 + a_{RP}C_e^g}$	[158]
	Sips isotherm model	$q_e = \frac{q_{ms}K_S C_e^{n_s}}{1 + K_S C_e^{n_s}}$	[159]
	Toth isotherm model	$q_e = \frac{K_T C_e}{(a_T + C_e^Z)^{1/z}}$	[160]
	Temkin isotherm model	$q_e = \frac{RT}{b}\ln(AC_e)$	[161]
Adsorption models based on Polanyi's potential theory	Dubinin-Radushkevich (D-R) isotherm model	$q_e = q_{mD-R}e^{-K_{DR}\varepsilon^2}$ $\varepsilon = RT\ln\frac{C_s}{C_e}$	[162]
	Dubinin-Astakhov (D-A) isotherm model	$q_e = q_{mD-A}e^{\left[-(\frac{\varepsilon}{E_{DA}})^{n_{DA}}\right]}$ $\varepsilon = RT\ln\frac{C_S}{C_e}$	[162]
Chemical adsorption models	Langmuir isotherm model	$q_e = \frac{q_m K_L C_e}{1 + K_L C_e}$	[163]
	Volmer isotherm model	$b_V C_e = \frac{q_e}{q_{mV} - q_e}e^{\frac{q_e}{q_{mV}-q_e}}$	[164]
Physical adsorption models	BET isotherm model (n ¼ ∞)	$q_e = \frac{q_{mBET}K_{BET}C_e}{(1 - K_{BET2}C_e)[1 - K_{BET2}C_e + K_{BE}}$	[165]
	Aranovich isotherm model	$q_e = \frac{q_{mA}C_A\frac{C_e}{C_{SA}}}{\sqrt{\left(1 - \frac{C_e}{C_{SA}}\right)}(1 + C_A\frac{C_e}{C_{SA}})}$	[166]
Ion exchange isotherm model	The homovalent ion exchange model	$\frac{c_A}{q_A} = \frac{1}{\xi}\left(c_A + \frac{c_B}{K_{B,A}}\right)$ $\frac{c_B}{q_B} = \frac{1}{\xi}\left(c_B + K_{B,\ A}c_A\right)$	[167]

	Monovalent and bivalent ions exchange model	$\frac{c_A}{q_A} = \frac{1}{\xi_{mono}}\left(c_A + \frac{2}{K_{B,A}}\frac{q_A\, c_B}{c_A}\right)$ $\frac{c_B}{q_B} = \frac{1}{\xi_{mono}}\left(2c_B + \frac{1}{K_{A,B}}\frac{c_A^2}{(\xi_{mono} - 2q_B)}\right)$	[168]

References

[1] Boretti A, Rosa L. Reassessing the projections of the World Water Development Report. Npj Clean Water 2019. https://doi.org/10.1038/s41545-019-0039-9.

[2] Gleick, Peter H. Lucy Allen, Michael J. Cohen HC, Juliet Christian-Smith, Matthew Heberger, Jason Morrison, Meena Palaniappan PS. The World's Water, The Biennial Report on Freshwater Resources. United States of America: 2012.

[3] Energy D, Elimelech M, Phillip WA. The Future of Seawater and the Environment. Science (80-) 2011;333:712–8.

[4] Elsaid K, Sayed ET, Yousef BAA, Kamal M, Rabaia H. Recent progress on the utilization of waste heat for desalination : A review. Energy Convers Manag 2020;221:113105. https://doi.org/10.1016/j.enconman.2020.113105.

[5] Duong HC, Ansari AJ, Hailemariam RH, Woo YC, Pham TM. Membrane Distillation for Strategic Water Treatment Applications : Opportunities, Challenges, and Current Status. Curr Pollut Reports 2020.

[6] OECD. OECD Environmental Outlook to 2050: The Consequences of Inaction. 2012.

[7] Shahzad MW, Burhan M, Ybyraiymkul D, Ng KC. Desalination Processes ' Efficiency and Future Roadmap. Entropy 2019. https://doi.org/10.3390/e21010084.

[8] Elsaid K, Sayed ET, Abdelkareem MA. Environmental Impact of Emerging Desalination Technologies: A preliminary Evaluation. J Environ Chem Eng 2020:37. https://doi.org/10.1016/j.jece.2020.104099.

[9] Lawal DU, Qasem NAA. Humidification-dehumidification desalination systems driven by thermal-based renewable and low-grade energy sources : A critical review. Renew Sustain

Energy Rev 2020;125:109817. https://doi.org/10.1016/j.rser.2020.109817.

[10] Mohammed RH, Askalany AA. Productivity Improvements of Adsorption Desalination Systems. Springer Singapore; 2019. https://doi.org/10.1007/978-981-13-6887-5.

[11] Goswami DY. Theoretical Analysis of a Water Desalination System Using Low Grade Solar Heat. Sol Energy Eng 2016;126. https://doi.org/10.1115/1.1669450.

[12] Li Z, Siddiqi A, Diaz L, Narayanamurti V. Towards sustainability in water-energy nexus : Ocean energy for seawater desalination. Renew Sustain Energy Rev 2017:0–1. https://doi.org/10.1016/j.rser.2017.10.087.

[13] Wang X, Ng KC. Experimental investigation of an adsorption desalination plant using low-temperature waste heat. Appl Therm Eng 2005;25:2780–9. https://doi.org/10.1016/j.applthermaleng.2005.02.011.

[14] D. Zejli, R. Benchrifa, A. Bennouna, O.K. Bouhelal. A solar adsorption desalination device: first simulation results. Desalination 2004;168:127–35.

[15] Taylor P. How Heat and Mass Recovery Strategies Impact the Performance of Adsorption Desalination Plant: Theory and Experiments. Heat Transf Eng n.d.:37–41. https://doi.org/10.1080/01457630601023625.

[16] Bouhal T, Fertahi S, Agrouaz Y, Rha T El, Kousksou T, Zeraouli Y, et al. Technical assessment, economic viability and investment risk analysis of solar heating / cooling systems in residential buildings in Morocco. Sol Energy 2018;170:1043–62. https://doi.org/10.1016/j.solener.2018.06.032.

[17] Thu K, Yanagi H, Baran B, Choon K. Performance investigation on a 4-bed adsorption desalination cycle with internal heat recovery scheme. DES 2017;402:88–96. https://doi.org/10.1016/j.desal.2016.09.027.

[18] Ng, KC and Wang, X and Gao, L and Chakraborty, A and Saha, BB and Koyama, S and Akisawa, A and Kashiwagi T. Apparatus and method for desalination, 2010.

[19] Saha BB, El-sharkawy II, Chakraborty A, Koyama S, Banker ND, Dutta P, et al. Evaluation of minimum desorption temperatures of thermal compressors in adsorption refrigeration cycles. Int J Refrig 2006;29. https://doi.org/10.1016/j.ijrefrig.2006.01.005.

[20] Srinivasan K, Dutta P, Baran B, Choon K. Realistic minimum desorption temperatures and compressor sizing for activated carbon þ HFC 134a adsorption coolers. Appl Therm Eng 2013;51:551–9. https://doi.org/10.1016/j.applthermaleng.2012.09.028.

[21] Sultan M. Performance evaluation of hydrophilic organic polymer sorbents for desiccant air-conditioning applications 2018. https://doi.org/10.1177/0263617417692338.

[22] Sultan M, Miyazaki T, Koyama S. Optimization of adsorption isotherm types for desiccant air-conditioning applications. Renew Energy 2018;121:441–50. https://doi.org/10.1016/j.renene.2018.01.045.

[23] Sultan M, El-sharkawy II, Miyazaki T, Baran B, Koyama S. An overview of solid desiccant dehumidificationand air conditioning systems. Renew Sustain Energy Rev 2015;46:16–29. https://doi.org/10.1016/j.rser.2015.02.038.

[24] Jani DB, Mishra M, Sahoo PK. Solid desiccant air conditioning – A state of the art review. Renew Sustain Energy Rev 2016;60:1451–69. https://doi.org/10.1016/j.rser.2016.03.031.

[25] Ge TS, Dai YJ, Wang RZ. Review on solar powered rotary desiccant wheel cooling system 2014;39:476–97. https://doi.org/10.1016/j.rser.2014.07.121.

[26] Choudhury B, Chatterjee PK, Sarkar JP. Review paper on solar-powered air-conditioning through adsorption route. Renew Sustain Energy Rev 2010;14:2189–95. https://doi.org/10.1016/j.rser.2010.03.025.

[27] Hamdy M, Askalany AA, Harby K, Kora N. An overview on adsorption cooling systems powered by waste heat from internal combustion engine. Renew Sustain Energy Rev 2015;51:1223–34. https://doi.org/10.1016/j.rser.2015.07.056.

[28] El-sharkawy II, Abdelmeguid H, Baran B. Potential application of solar powered adsorption cooling systems in the Middle East. Appl Energy 2014;126:235–45. https://doi.org/10.1016/j.apenergy.2014.03.092.

[29] Hassan HZ, Mohamad AA. A review on solar cold production through absorption technology. Renew Sustain Energy Rev 2012;16:5331–48. https://doi.org/10.1016/j.rser.2012.04.049.

[30] Zhai XQ, Qu M, Li Y, Wang RZ. A review for research and new design options of solar absorption cooling systems 2011;15:4416–23. https://doi.org/10.1016/j.rser.2011.06.016.

[31] Kalkan N, Young EA, Celiktas A. Solar thermal air conditioning technology reducing the footprint of solar thermal air conditioning. Renew Sustain Energy Rev 2012;16:6352–83. https://doi.org/10.1016/j.rser.2012.07.014.

[32] Shabir F, Sultan M, Niaz Y, Usman M, Ibrahim SM. Steady-State Investigation of Carbon-Based Adsorbent–Adsorbate Pairs for Heat Transformation Application 2020.

https://doi.org/10.3390/su12177040.
[33] Broughton, Donald B. (Des Plaines I. Continuous desalination process. 06/503490, 1984.
[34] Alsaman AS, Askalany AA, Harby K, Ahmed MS. A state of the art of hybrid adsorption desalination – cooling systems. Renew Sustain Energy Rev 2016;58:692–703. https://doi.org/10.1016/j.rser.2015.12.266.
[35] Saha BB, El-sharkawy II, Shahzad MW, Thu K, Ng KC. Fundamental and application aspects of adsorption cooling and desalination. Elsevier n.d.
[36] Askalany AA. Innovative mechanical vapor compression adsorption desalination (MVC-AD) system. Appl Therm Eng 2016. https://doi.org/10.1016/j.applthermaleng.2016.05.144.
[37] Mohammed RH, Mesalhy O, Elsayed ML, Chow LC. Performance evaluation of a new modular packed bed for adsorption cooling systems. Appl Therm Eng 2018. https://doi.org/10.1016/j.applthermaleng.2018.02.103.
[38] Mohammed RH, Mesalhy O, Elsayed ML, Chow LC. Scaling analysis of heat and mass transfer processes in an adsorption packed bed. Int J Therm Sci 2018;133:82–9. https://doi.org/10.1016/j.ijthermalsci.2018.07.017.
[39] Mohammed RH, Mesalhy O, Elsayed ML, Su M, Chow LC. Revisiting the adsorption equilibrium equations of silica gel/water for adsorption cooling applications. Int J Refrig 2017. https://doi.org/10.1016/j.ijrefrig.2017.10.038.
[40] Amirfakhraei A, Zarei T, Khorshidi J. Performance improvement of adsorption desalination system by applying mass and heat recovery processes. Therm Sci Eng Prog 2020;18:100516. https://doi.org/10.1016/j.tsep.2020.100516.
[41] Thu K, Choon K, Saha BB, Chakraborty A, Koyama S. Operational strategy of adsorption desalination systems. Int J Heat Mass Transf 2009;52:1811–6. https://doi.org/10.1016/j.ijheatmasstransfer.2008.10.012.
[42] Rahimi-ahar Z, Sadegh M, Rahimi L. Air Humidification-Dehumidification Process for Desalination : A review. Prog Energy Combust Sci 2020;80. https://doi.org/10.1016/j.pecs.2020.100850.
[43] Thu K. ADSORPTION DESALINATION : THEORY & EXPERIMENTS. 2010.
[44] El-sharkawy II, Ng KC, Saha BB. Performance improvement of adsorption desalination plant: experimental investigation. Int Rev Mech Eng 2007;1.

[45] Ng KC, Thu K, Yanagi H, Saha BB, Chakraborty A, Al-Ghasham, Tawfiq Y. APPARATUS AND METHOD FOR IMPROVED DESALINATION, 2009.

[46] Choon K, Wang X, Sern Y, Baran B, Chakarborty A, Koyama S, et al. Experimental study on performance improvement of a four-bed adsorption chiller by using heat and mass recovery 2006;49:3343–8. https://doi.org/10.1016/j.ijheatmasstransfer.2006.01.053.

[47] Thu K, Baran B, Chakraborty A, Gee W, Choon K. Study on an advanced adsorption desalination cycle with evaporator–condenser heat recovery circuit. Int J Heat Mass Transf 2011;54:43–51. https://doi.org/10.1016/j.ijheatmasstransfer.2010.09.065.

[48] Thu K, Chakraborty A, Kim Y, Myat A, Baran B, Choon K. Numerical simulation and performance investigation of an advanced adsorption desalination cycle. DES 2013;308:209–18. https://doi.org/10.1016/j.desal.2012.04.021.

[49] Taylor P, Thu K, Kim Y, Myat A, Chakraborty A, Ng KC. Performance investigation of advanced adsorption desalination cycle with condenser–evaporator heat recovery scheme 2013:37–41. https://doi.org/10.1080/19443994.2012.693659.

[50] Ng KC, Thu K, Shahzad MW, Chun W. Progress of adsorption cycle and its hybrids with conventional multi-effect desalination processes. J Desalin Water Reuse 2014;6. https://doi.org/10.1179/2051645214Y.0000000020.

[51] Shahzad MW, Burhan M, Ng KC. OPEN A standard primary energy approach for comparing desalination processes. Npj Clean Water 2019:1–7. https://doi.org/10.1038/s41545-018-0028-4.

[52] Darwish MA. Thermal Analysis of Multi-Stage Flash Desalting Systems. Desalination 1991;85:59–79.

[53] Splegler KS, E-sayed YM. The energetics of desalination processes. Desalination 2001;134:109–28.

[54] P Abhishek VB. Thermodynamic modelling of hybrid adsorption system 2019. https://doi.org/10.1088/1742-6596/1355/1/012013.

[55] Wu JW. A Study of Silica Gel Adsorption Desalination System. 2012.

[56] Ng KC, Chua HT, Chung CY, Loke CH, Kashiwagi T. Experimental investigation of the silica gel ± water adsorption isotherm characteristics. Appl Therm Eng 2001;21.

[57] Chakraborty A, Saha BB, Koyama S, Ng KC, Srinivasan K, Framework T. Adsorption Thermodynamics of Silica Gel - Water Systems. J Chem Eng Data 2009:448–52.

[58] Amin M, Shahmirzadi A, Saeid S, Luo J. Significance, evolution and recent advances in adsorption technology, materials and processes for desalination, water softening and salt removal. J Environ Manage 2018;215:324–44. https://doi.org/10.1016/j.jenvman.2018.03.040.

[59] Choon K, Thu K, Kim Y, Chakraborty A, Amy G. Adsorption desalination : An emerging low-cost thermal desalination method. Desalination 2013;308:161–79. https://doi.org/10.1016/j.desal.2012.07.030.

[60] Shahzad MW, Burhan M, Ang L, Ng KC. Adsorption desalination— Principles, process design, and its hybrids for future sustainable desalination. Elsevier Inc.; 2018. https://doi.org/10.1016/B978-0-12-815818-0.00001-1.

[61] Wang LW, Wang RZ, Oliveira RG. A review on adsorption working pairs for refrigeration 2009;13:518–34. https://doi.org/10.1016/j.rser.2007.12.002.

[62] Wang LW, Wang RZ, Wu JY, Wang K, Wang SG. Adsorption ice makers for fishing boats driven by the exhaust heat from diesel engine : choice of adsorption pair 2004;45:2043–57. https://doi.org/10.1016/j.enconman.2003.10.021.

[63] Wang LW, Wang RZ, Wu JY, Wang K. Compound adsorbent for adsorption ice maker on fishing boats 2004;27:401–8. https://doi.org/10.1016/j.ijrefrig.2003.11.010.

[64] Groll M. REACTION BEDS FOR DRY SORPTION MACHINES 1993;13:341–6.

[65] Crozat G, Mauran S. GASEOUS-SOLID REACTION 1986:2–5.

[66] Jribi S, Miyazaki T, Baran B, Pal A, Younes MM. Equilibrium and kinetics of CO2 adsorption onto activated carbon. Int J Heat Mass Transf 2017;108:1941–6. https://doi.org/10.1016/j.ijheatmasstransfer.2016.12.114.

[67] Mauran S, Paades P, Haridon FL. HEAT AND MASS TRANSFER IN CONSOLIDATED REACTING BEDS FOR THERMOCHEMICAL SYSTEMS 1993;13:315–9.

[68] Aidoun Z, Ternan M. Synthesis of a nanostructured pillar MOF with high adsorption capacitytowards antibiotics pollutants from aqueous solution 2002;22:1163–73.

[69] Sultan M, Miyazaki T, Baran B, Koyama S. Steady-state investigation of water vapor adsorption for thermally driven adsorption based greenhouse air-conditioning system. Renew Energy 2016;86:785–95. https://doi.org/10.1016/j.renene.2015.09.015.

[70] Thu K, Chakraborty A, Baran B, Choon K. Thermo-physical properties of silica gel for

adsorption desalination cycle. Appl Therm Eng 2013;50:1596–602. https://doi.org/10.1016/j.applthermaleng.2011.09.038.
[71] Myat A, Kim N, Thu K, Kim Y. Experimental investigation on the optimal performance of Zeolite – water adsorption chiller. Appl Energy 2013;102:582–90. https://doi.org/10.1016/j.apenergy.2012.08.005.
[72] Thu K, Yanagi H, Baran B, Choon K. Performance analysis of a low-temperature waste heat-driven adsorption desalination prototype. Int J Heat Mass Transf 2013;65:662–9. https://doi.org/10.1016/j.ijheatmasstransfer.2013.06.053.
[73] Youssef PG, Mahmoud SM, Al-dadah RK. Numerical simulation of combined adsorption desalination and cooling cycles with integrated evaporator / condenser. Desalination 2016;392:14–24. https://doi.org/10.1016/j.desal.2016.04.011.
[74] Burhan M, Shahzad MW, Ng KC. Energy distribution function based universal adsorption isotherm model for all types of isotherm 2018. https://doi.org/10.1093/ijlct/cty031.
[75] Miyazaki T, Miyawaki J, Ohba T, Yoon S. Study Toward High-Performance Thermally Driven Air-Conditioning Systems 2017;020002. https://doi.org/10.1063/1.4968250.
[76] Sultan M, Miyazaki T, Saha BB, Koyama S, Kil H, Nakabayashi K, et al. Adsorption of Difluoromethane (HFC-32) onto phenol resin based adsorbent: Theory and experiments. Int J Heat Mass Transf 2018;127:348–56. https://doi.org/10.1016/j.ijheatmasstransfer.2018.07.097.
[77] SAHA BB, Ibrahim I, Wakil M, Choon K. Fundamental and application aspects of adsorption cooling and desalination. Appl Therm Eng 2015. https://doi.org/10.1016/j.applthermaleng.2015.09.113.
[78] Anutosh Chakraborty, Kai Choong Leong, Kyaw Thu, Bidyut Baran Saha and KCN. Theoretical insight of adsorption cooling. Appl Phys Lett Arch 2020. https://doi.org/10.1063/1.3592260.
[79] Choon K, Thu K, Baran B, Chakraborty A. Study on a waste heat-driven adsorption cooling cum desalination cycle. Int J Refrig 2011;35:685–93. https://doi.org/10.1016/j.ijrefrig.2011.01.008.
[80] Wang X, Zimmermann W, Ng KC, Chakraboty A, Keller JU. INVESTIGATION ON THE ISOTHERM OF SILICA GEL + WATER SYSTEMS TG and volumetric methods 2004;76:659–69.

[81] Wei H, Teo B, Chakraborty A, Han B. Water Adsorption on CHA and AFI Types Zeolites: Modelling and Investigation of Adsorption Chiller under Static and Dynamic Conditions. Appl Therm Eng 2017. https://doi.org/10.1016/j.applthermaleng.2017.08.014.

[82] Mobedi M, Ülkü S. Effect of regeneration temperature on adsorption equilibria and mass diffusivity of zeolite 13x-water pair 2016;224. https://doi.org/10.1016/j.micromeso.2015.10.041.

[83] Chakraborty A, Thu K, Saha BB, Ng C. Adsorption – Desalination Cycle. Adv. Water Desalin., 2013, p. 377–451.

[84] Saha BB, El-sharkawy II, Shahzad MW, Thu K, Ang L, Ng KC. Fundamental and application aspects of adsorption cooling and desalination. Appl Therm Eng 2015. https://doi.org/10.1016/j.applthermaleng.2015.09.113.

[85] Taylor P, Martínez A, Uche J, Rubio C, Carrasquer B. Desalination and Water Treatment Exergy cost of water supply and water treatment technologies. Desalin Water Treat 2012:37–41. https://doi.org/10.5004/dwt.2010.1368.

[86] Mabrouk AA, Nafey AS, Fath HES. Steam , electricity and water costs evaluation of power desalination co- generation plants. Desalin Water Treat 2010;22:56–64. https://doi.org/10.5004/dwt.2010.1537.

[87] Sadri S, Ameri M, Khoshkhoo RH. A new approach to thermo-economic modeling of adsorption desalination system. Desalination 2018;428:69–75. https://doi.org/10.1016/j.desal.2017.11.027.

[88] Vasilescu EE. Exergy analysis of an adsorption refrigeration machine. Int J Exergy 2007;4.

[89] Adrian Bejan, George Tsatsaronis MJM. Thermal Design and Optimization. 1995.

[90] Chakraborty A, Baran B, Aristov YI. Dynamic behaviors of adsorption chiller: Effects of the silica gel grain size and layers. Energy 2014. https://doi.org/10.1016/j.energy.2014.10.015.

[91] Youssef PG, Mahmoud SM, Al-dadah RK. Performance analysis of four bed adsorption water desalination/refrigeration system, comparison of AQSOA-Z02 to silica gel 2019. https://doi.org/10.1016/j.desal.2015.08.002.

[92] Wakil M, Choon K, Thu K, Baran B. Multi effect desalination and adsorption desalination (MEDAD): A hybrid desalination method. Appl Therm Eng 2014.

https://doi.org/10.1016/j.applthermaleng.2014.03.064.

[93] Ng KC, Thu K, Chakraborty A, Saha BB, Chun WG, Korea S. Solar-assisted dual-effect adsorption cycle for the production of cooling effect and potable water 2009:61–7. https://doi.org/10.1093/ijlct/ctp008.

[94] Thu K, Chakraborty A, Kim Y, Myat A, Baran B, Choon K. Numerical simulation and performance investigation of an advanced adsorption desalination cycle. Desalination 2013;308:209–18. https://doi.org/10.1016/j.desal.2012.04.021.

[95] Ali ES, Askalany AA, Harby K, Diab MR, Alsaman AS. Adsorption desalination-cooling system employing copper sulfate driven by low grade heat sources. Appl Therm Eng 2018. https://doi.org/10.1016/j.applthermaleng.2018.03.014.

[96] Taylor P, Ng KC, Saha BB, Chakraborty A, Koyama S. Adsorption Desalination Quenches Global Thirst. Heat Transf Eng 2011:37–41. https://doi.org/10.1080/01457630802125310.

[97] Wu JW, Biggs MJ, Hu EJ. Dynamic model for the optimisation of adsorption-based desalination processes. Appl Therm Eng 2014;66:464–73. https://doi.org/10.1016/j.applthermaleng.2014.02.045.

[98] Youssef PG, Al-dadah RK, Mahmoud SM, Dakkama HJ, Elsayed A. Effect of Evaporator and Condenser Temperatures on the Performance of Adsorption Desalination Cooling Cycle. Energy Procedia 2015;75:1464–9. https://doi.org/10.1016/j.egypro.2015.07.263.

[99] Mitra S, Thu K, Saha BB, Srinivasan K, Dutta P. Modeling study of two-stage , multi-bed air cooled silica gel + water adsorption cooling cum desalination system. Appl Therm Eng 2016. https://doi.org/10.1016/j.applthermaleng.2016.12.011.

[100] Alsaman AS, Askalany AA, Harby K, Ahmed MS. Performance evaluation of a solar-driven adsorption desalination-cooling system. Energy 2017. https://doi.org/10.1016/j.energy.2017.04.010.

[101] Elsayed E, Al-dadah R, Mahmoud S, Anderson PA, Elsayed A, Youssef PG. CPO-27 (Ni), aluminium fumarate and MIL-101 (Cr) MOF materials for adsorption water desalination. DES 2016;27. https://doi.org/10.1016/j.desal.2016.07.030.

[102] Youssef PG, Dakkama H, Mahmoud SM, Al-dadah RK. Experimental investigation of adsorption water desalination/cooling system using CPO-27Ni MOF. Desalination 2017;404:192–9. https://doi.org/10.1016/j.desal.2016.11.008.

[103] Askalany AA, Ali ES. A new approach integration of ejector within adsorption desalination cycle reaching COP higher than one. Sustain Energy Technol Assessments 2020;41:100766. https://doi.org/10.1016/j.seta.2020.100766.

[104] Elbassoussi MH, Mohammed RH, Zubair SM. Thermoeconomic assessment of an adsorption cooling / desalination cycle coupled with a water-heated humidification-dehumidification desalination unit. Energy Convers Manag 2020;223:113270. https://doi.org/10.1016/j.enconman.2020.113270.

[105] Thimmaiah PC, Sharafian A, Rouhani M, Huttema W, Bahrami M. Evaluation of low-pressure flooded evaporator performance for adsorption chillers. Energy 2017. https://doi.org/10.1016/j.energy.2017.01.085.

[106] Rezk ARM, Al-dadah RK. Physical and operating conditions effects on silica gel/water adsorption chiller performance. Appl Energy 2012;89:142–9. https://doi.org/10.1016/j.apenergy.2010.11.021.

[107] Al-Alili A, Islam MD, Kubo I, Hwang Y, Radermacher R. Modeling of a solar powered absorption cycle for Abu Dhabi. Appl Energy 2012;93:160–7. https://doi.org/10.1016/j.apenergy.2010.11.034.

[108] Saha BB, Chakraborty A, Koyama S, Srinivasan K, Ng KC, Dutta P, et al. Thermodynamic formalism of minimum heat source temperature for driving advanced adsorption cooling device 2014;111902:26–9. https://doi.org/10.1063/1.2780117.

[109] Askalany A, Ali ES, Mohammed RH. A novel cycle for adsorption desalination system with two stages-ejector for higher water production and efficiency. Desalination 2020;496:114753. https://doi.org/10.1016/j.desal.2020.114753.

[110] Huang BJ, Chang JM, Wang CP, Petrenko VA. A 1-D analysis of ejector performance 1999;22:354–64.

[111] Askalany AA, Ernst S, Henninger SK, Alsaman AS, Ernst S, Henninger SK, et al. High potential of employing bentonite in adsorption cooling systems driven by low grade heat source temperatures 2017. https://doi.org/10.1016/j.energy.2017.07.171.

[112] Yan J, Cai W, Zhao L, Li Y, Lin C. Performance evaluation of a combined ejector-vapor compression cycle. Renew Energy 2013;55:331–7. https://doi.org/10.1016/j.renene.2012.12.029.

[113] Megdouli K, Tashtoush BM, Nahdi E, Elakhdar M, Mhimid A, Kairouani L. Performance

analysis of a combined vapor compression cycle and ejector cycle for refrigeration cogeneration. Int J Refrig 2016. https://doi.org/10.1016/j.ijrefrig.2016.12.003.

[114] Liang X, Zhou S, Deng J, He G, Cai D. Thermodynamic analysis of a novel combined double ejector- absorption refrigeration system using ammonia / salt working pairs without mechanical pumps. Energy 2019;185:895–909. https://doi.org/10.1016/j.energy.2019.07.104.

[115] Majdi HS. Performance evaluation of combined ejector LiBr/H2O absorption cooling cycle. Case Stud Therm Eng 2016;7:25–35. https://doi.org/10.1016/j.csite.2016.01.003.

[116] Mohammed RH, Askalany AA. Productivity Improvements of Adsorption Desalination Systems of Adsorption Desalination Systems. 2019. https://doi.org/10.1007/978-981-13-6887-5.

[117] Wu JW, Hu EJ, Biggs MJ. Thermodynamic analysis of an adsorption-based desalination cycle (part II): Effect of evaporator temperature on performance. Chem Eng Res Des 2011;89:2168–75. https://doi.org/10.1016/j.cherd.2010.12.012.

[118] Yong L, Wang RZ. Adsorption Refrigeration: A Survey of Novel Technologies. Recent Patents Eng 2007;1:1–21.

[119] Mitra S, Srinivasan K, Kumar P, Murthy SS, Dutta P. Solar driven Adsorption Desalination system. Energy Procedia 2014;49:2261–9. https://doi.org/10.1016/j.egypro.2014.03.239.

[120] Rahul Raj, V.Baiju. Thermodynamic Analysis of a Solar Powered Adsorption Cooling and Desalination System. Energy Procedia 2019;158:885–91. https://doi.org/10.1016/j.egypro.2019.01.226.

[121] Kim Y, Thu K, Masry ME, Choon K. Water quality assessment of solar-assisted adsorption desalination cycle. DES 2014;344:144–51. https://doi.org/10.1016/j.desal.2014.03.021.

[122] Lemmini F, Errougani A. Building and experimentation of a solar powered adsorption refrigerator. Renew Energy 2005;30:1989–2003. https://doi.org/10.1016/j.renene.2005.03.003.

[123] Ahmadi M, Thimmaiah P. Experimental and numerical investigation of a solar eductor-assisted low-pressure water desalination system. Sci Bull 2016;61:959–73. https://doi.org/10.1007/s11434-016-1092-0.

[124] Al-Karaghouli A, L.Kazmerski L. Energy consumption and water production cost of conventional and renewable-energy-powered desalination processes. Renew Sustain Energy Rev 2013;24:343–56. https://doi.org/10.1016/j.rser.2012.12.064.

[125] Ang WS, Yip NY, Tiraferri A, Elimelech M. Chemical cleaning of RO membranes fouled by wastewater effluent : Achieving higher efficiency with dual-step cleaning. J Memb Sci 2011;382:100–6. https://doi.org/10.1016/j.memsci.2011.07.047.

[126] Ou R, Zhang H, Truong VX, Zhang L, Hegab HM, Han L, et al. A sunlight-responsive metal–organic framework system for sustainable water desalination. Nat Sustain 2020. https://doi.org/10.1038/s41893-020-0590-x.

[127] Burn S, Hoang M, Zarzo D, Olewniak F, Campos E, Bolto B, et al. Desalination techniques — A review of the opportunities for desalination in agriculture. DES 2015;364:2–16. https://doi.org/10.1016/j.desal.2015.01.041.

[128] Chandrasekara NPGN, Pashley RM. Study of a new process for the efficient regeneration of ion exchange resins. DES 2015;357:131–9. https://doi.org/10.1016/j.desal.2014.11.024.

[129] Sludak R, Weiss DE. An ion exchange process with thermal regeneration IX. A new type of rapidly reacting ion-exchange resin☆. Desalination 1973;3:269–85.

[130] Ou R, Zhang H, Wei J, Kim S, Wan L, Nguyen NS, et al. Thermoresponsive Amphoteric Metal–Organic Frameworks for Efficient and Reversible Adsorption of Multiple Salts from Water. Adv Mater 2018;1802767:1–8. https://doi.org/10.1002/adma.201802767.

[131] Shahzad MW, Burhan M, Gha N, Ng KC. A multi evaporator desalination system operated with thermocline energy for future sustainability 2017. https://doi.org/10.1016/j.desal.2017.04.013.

[132] Soo H, Wakil M, Ghaffour N, Choon K. Pilot studies on synergetic impacts of energy utilization in hybrid desalination system : Multi-effect distillation and adsorption cycle (MED-AD). Desalination 2020;477:114266. https://doi.org/10.1016/j.desal.2019.114266.

[133] Sharafian A, Dan PC, Huttema W, Bahrami M. Performance analysis of a novel expansion valve and control valves designed for a waste heat-driven two-adsorber bed adsorption cooling system. Appl Therm Eng 2016;100:1119–29. https://doi.org/10.1016/j.applthermaleng.2016.02.118.

[134] Shara A, Mahdi S, Mehr N, Thimmaiah PC, Huttema W, Bahrami M. Effects of adsorbent mass and number of adsorber beds on the performance of a waste heat-driven adsorption

cooling system for vehicle air conditioning applications 2016;112. https://doi.org/10.1016/j.energy.2016.06.099.

[135] Abid A, Ahmad M, Umer M, Yaqoob H, Ali L, Wakil M. Exergoeconomic optimization of a forward feed multi-effect desalination system with and without energy recovery. Desalination 2021;499:114808. https://doi.org/10.1016/j.desal.2020.114808.

[136] Sayyaadi H, Saffari A. Thermoeconomic optimization of multi effect distillation desalination systems. Appl Energy 2010;87:1122–33. https://doi.org/10.1016/j.apenergy.2009.05.023.

[137] Shu L, Chen L, Sun F. Performance optimization of a diabatic distillation-column by allocating a sequential heat-exchanger inventory 2007;84:893–903. https://doi.org/10.1016/j.apenergy.2007.02.003.

[138] Huang Y, Khajepour A, Bagheri F, Bahrami M. Optimal energy-efficient predictive controllers in automotive air- conditioning / refrigeration systems. Appl Energy 2016;184:605–18. https://doi.org/10.1016/j.apenergy.2016.09.086.

[139] Alarcón-padilla D, García-rodríguez L. Application of absorption heat pumps to multi-effect distillation : a case study of solar desalination 2007;212:294–302. https://doi.org/10.1016/j.desal.2006.10.014.

[140] Ettouney, El-Dessouky HT, M. H. Multiple Effect Evaporation Vapor Compression. Fundam. Salt Water Desalin., 2002, p. 690. https://doi.org/https://doi.org/10.1016/B978-0-444-50810-2.X5000-3.

[141] Alarcón-padilla DC, García-rodríguez L, Blanco-gálvez J. Experimental assessment of connection of an absorption heat pump to a multi-effect distillation unit. DES 2010;250:500–5. https://doi.org/10.1016/j.desal.2009.06.056.

[142] Alarcón-padilla DC, García-rodríguez L, Blanco-gálvez J. Design recommendations for a multi-effect distillation plant connected to a double-effect absorption heat pump : A solar desalination case study. DES 2010;262:11–4. https://doi.org/10.1016/j.desal.2010.04.064.

[143] Wang Y, Lior N. Proposal and analysis of a high-efficiency combined desalination and refrigeration system based on the LiBr–H2O absorption cycle—Part 2: Thermal performance analysis and discussions. Energy Convers Manag 2011;52:228–35. https://doi.org/10.1016/j.enconman.2010.06.064.

[144] Wang Y, Lior N. Thermoeconomic analysis of a low-temperature multi-effect thermal

desalination system coupled with an absorption heat pump. Energy 2011;36:3878–87. https://doi.org/10.1016/j.energy.2010.09.028.

[145] Chen Q, Muhammad B, Hassan F, Ybyraiymkul D, Shahzad W, Li Y, et al. Thermo-economic analysis and optimization of a vacuum multi-effect membrane distillation system. Desalination 2020;483:114413. https://doi.org/10.1016/j.desal.2020.114413.

[146] Wakil M, Choon K. An Emerging Hybrid Multi-Effect Adsorption Desalination System 2014;1:30–6.

[147] Ng KC, WANG XL, GAO L, CHAKRABORTY A, Saha BB, KOYAMA S, et al. APPARATUS AND METHOD FOR DESALINATION, 2005.

[148] Shahzad W, Ybyraiymkul D, Ybyraiymkul D, Shahzad MW. Renewable Energy-Driven Desalination Hybrids for Sustainability Sustainability 2018. https://doi.org/10.5772/intechopen.77019.

[149] Shahzad MW, Burhan M, Ng KC. Renewable Energy Storage and Its Application for Desalination 2019:313–29.

[150] Wakil M, Ybyraiymkul D, Burhan M. An innovative pressure swing adsorption cycle. AIP Conf Proc 2062 2019;020057. https://doi.org/10.1063/1.5086604.

[151] Taylor P, Thu K, Chakraborty A, Saha BB, Chun WG, Ng KC. Life-cycle cost analysis of adsorption cycles for desalination n.d.:37–41. https://doi.org/10.5004/dwt.2010.1187.

[152] Saha BB, Ng KC, Chakraborty A, Kyaw T. Most energy efficient approach of desalination and cooling. Cool India 2009.

[153] Fayazmanesh K, Mccague C, Bahrami M. Consolidated adsorbent containing graphite flakes for heat-driven water sorption cooling systems. Appl Therm Eng 2017;123:753–60. https://doi.org/10.1016/j.applthermaleng.2017.05.114.

[154] Ghaffour N, Lattemann S, Missimer T, Choon K, Sinha S, Amy G. Renewable energy-driven innovative energy-efficient desalination technologies. Appl Energy 2014:1–11. https://doi.org/10.1016/j.apenergy.2014.03.033.

[155] Anutosh Chakraborty, Kyaw Thu, Bidyut Baran Saha, Kim Choon Ng. Advances in water desalination. John Wiley & Sons; 2012.

[156] Wang J, Guo X. Adsorption isotherm models: Classification, physical meaning, application and solving method. Chemosphere 2020;258:127279. https://doi.org/10.1016/j.chemosphere.2020.127279.

[157] Freundlich H. Über die Adsorption in Lösungen. Zeitschrift für Physikalische Chemie; 1906.

[158] Redlich O, Peterson DL. A Useful Adsorption Isotherm. J Phys Chem 1959;6:1024–6.

[159] Sips R. On the Structure of a Catalyst Surface. J Chem Phys 1948;16:490. https://doi.org/10.1063/1.1746922.

[160] Tóth J. State Equation of the Solid-Gas Interface Layers. Mater Sci 1971;69.

[161] Temkin M, Pyzhev V. Kinetics of Ammonia Synthesis on Promoted Iron Catalysts. Temkin, M Pyzhev, V 1940;12.

[162] Dubinin MM, Radushkevich LV. The Equation of the Characteristic Curve of Activated Charcoal. Proc USSR Acad Sci Phys Chem Sect 55 1971:331–7.

[163] Langmuir I. The Constitution and Fundamental Properties of Solids and Liquids. II Liquids. J Am Chem Soc 1917;39.

[164] Volmer M. Thermodynamische Folgerungen ans der Zustandsgleichnng für adsorbierte Stoffe. Zeitschrift Für Phys Chemie 1925;115.

[165] BRUNAUER S, EMMETT PH, TELLER E. Adsorption of Gases in Multimolecular Layers. J Am Chem Soc 1938;60:309–319.

[166] Aranovich GL. The Theory of Polymolecular Adsorption. Langmuir 1992;8:736–9.

[167] Kónya J, Nagy NM. Isotherm equation of sorption of electrolyte solutions on solids: how to do heterogeneous surface from homogeneous one? Period Polytech 2009;53:55–60.

[168] Nagy NM, Kova´cs EM, Ko´nya J. Ion exchange isotherms in solid: electrolyte solution systems. J Radioanal Nucl Chem 2016;308:1017–26. https://doi.org/10.1007/s10967-015-4536-0.